Review of Yang et al., Transport of volcanic aerosol from the Raikoke eruption in 2019 through the Northern Hemisphere

Original referee comments are in blue.

Our responses are in black with regular bold format. Text from the updated manuscript:

Appears in italic and with 0.5 cm indentation and with the modified parts in red.

General comments

The submitted manuscript uses aerosol profiles measurements made by COBALD sondes at Lhasa and POPS at Boulder to study the distribution of aerosol from the Raikoke volcanic eruption in June 2019, particularly within the Asian Summer Monsoon Anticyclone but also including transport to Boulder.

Firstly, back trajectories are used to study the transport pathways to Lhasa, and then in the second part, the CLaMS model is used to try to simulate the profiles after injection of an SO2 tracer. (Not including the upper peak seen in the COBALD and POPS profiles around 470-480 K).

The model shows a reasonable ability to reproduce the observed results and some interesting sensitivity studies are also performed to try to obtain the best possible agreement and assess model settings.

Overall this is an interesting and worthwhile study about an important topic and well within the scope of ACP, and I would be happy to recommend publication after some minor improvements.

The presentation is generally very clear and well-written with a small number of exceptions listed below.

To me, the agreement of the model and observations seems only modestly good so I would suggest a small amount of additional text in the discussion section or conclusions to put these results into context and how happy you were with them.

I also note that the CLaMS simulations did not attempt to model the upper peak seen in Figure 2 and Figure 8 which seems disappointing, so some comment about that would also be welcome.

We thank the reviewer for the encouraging assessment and the detailed, constructive comments, which helped us improve the manuscript.

Regarding the upper peak (Lhasa on 3 August; Boulder on 27 August), we agree that the current CLaMS set-up does not reproduce this feature by the SO_2-based tracer fraction profile like shown in the Fig. 9 and Fig. 11 in the revised manuscript. Indeed, on 12 July 2019 a condensed VVP structure can be identified in TROPOMI observations (as shown in Fig. 1 of this reply). We performed an additional CLaMS three-dimensional SO_2-based tracer sensitivity simulation by injecting tracer at 00:00 UTC on 12 July in the 440–460 K layer and analyzing the subsequent tracer fraction distribution (as shown in Figs. 1 and 2 of this reply). Although this run does not create a distinct additional peak in the simulated SO_2-based tracer fraction profiles, it yields enhanced tracer fractions near the observation times/locations

(Lhasa on 3 August; Boulder on 27 August). We therefore infer that the filament transport is broadly consistent with the observations. However, due to the fact that the filament is highly localized and small-scale, the current CLaMS simulation is not able to fully capture the feature with the given model resolution

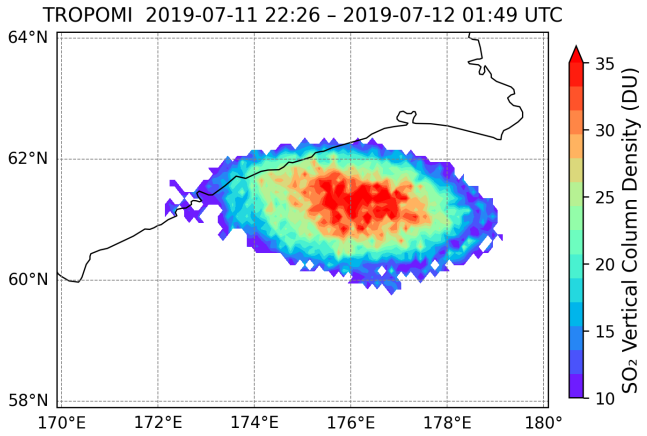

Figure 1. TROPOMI SO_2 total vertical column showing the condensed vorticized volcanic plume (VVP) from the 2019 Raikoke eruption during 11 July 2019 22:26 to 12 July 2019 01:49 UTC.

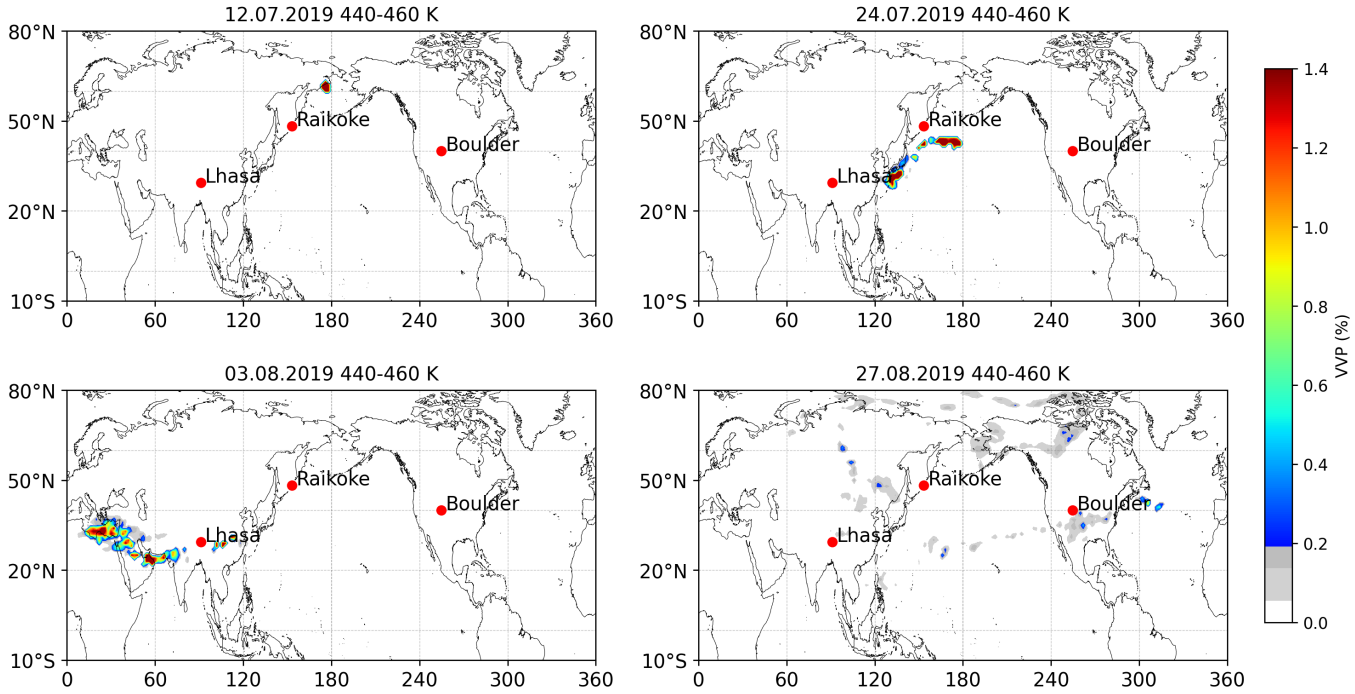

Figure 2. Four maps of CLaMS SO_2-based tracer fraction (%) averaged over 440 to 460 K at 00:00 UTC on 12 July, 24 July, 3 August, and 27 August 2019, using the injection SO_2 mask from Fig. 1. Red markers indicate the location of Raikoke, Lhasa, and Boulder.

Specific comments

Lines 19, 34 – this is a very minor comment, but I am not aware of much discussion of volcanic injection of water vapor prior to Hunga.

We agree and revised the text to avoid implying that substantial water-vapour injection into the UTLS/stratosphere is common for large eruptions. The discussion now emphasizes SO_2

and ash as the primary injected species, and mentions stratospheric water vapour impacts only as an exceptional case (e.g. the 2022 Hunga Tonga eruption).

Large eruptions can inject significant amounts of ash~~, water vapor,~~ and sulfur dioxide (SO_2) into the upper troposphere–lower stratosphere (UTLS).

~~The Volcanic Explosivity Index (VEI) serves as a proxy for eruption intensity (Newhall and Self, 1982), and events with VEI ≥ 4 can inject vast quantities of SO2, water vapor, and ash, causing marked climate perturbations.~~ Eruption magnitude can be characterized by the amount of SO_2 and ash released, which largely controls aerosol formation potential and radiative forcing. Notably, substantial perturbations of stratospheric water vapour and aerosol microphysics have also been reported for the 2022 Hunga Tonga eruption despite modest SO_2 injection (Carn et al., 2022; Zhu et al., 2022).

Lines 39-41 The wording implies there are other examples of this in the record apart from Hunga?

We agree that the previous wording could be interpreted as implying multiple examples. We have revised the text to clearly refer to the 2022 Hunga Tonga eruption as the illustrative case for pronounced stratospheric water vapour perturbations

Lines 44-46 These sentences need some minor re-wording for clarity. It is hard for the reader to understand "… the circulation acts as a … barrier, trapping those air masses … Simultaneously, the barrier is permeable … This dual role … ". This reads like a superposition of contradictory states.

We agree that the text might be somewhat confusing and rewrote the respective paragraph to enhance clarity as follows:

~~Among the various transport mechanisms influencing volcanic aerosol fate, the ASMA plays a particularly important role during the boreal summer. Deep convection injects pollutants into the UTLS, where the ASMA's strong anticyclonic circulation acts as a dynamical transport barrier, trapping those air masses in its circulation. Simultaneously, the barrier is permeable, and the horizontal outflow of the ASMA can transport monsoon air masses to the extratropical UTLS (Vogel et al., 2016; Yu et al., 2017). This dual role makes the ASMA a key element in understanding aerosol dispersion in the Northern Hemisphere following volcanic eruptions.~~ In the Northern Hemisphere summer, the ASMA is the dominant circulation system in the UTLS. Deep convection injects pollutants into the UTLS, where the ASMA's strong anticyclonic circulation acts as a dynamical transport barrier that confines these air masses over Asia during their ascent into the stratosphere (e.g., Park et al., 2007; Randel et al., 2010; Fadnavis et al., 2014; Santee et al., 2017; Vogel et al., 2019). However, the ASMA boundary is not a strict barrier, and air masses can be exported from the monsoon circulation into the extratropical UTLS (Vogel et al., 2016; Yu et al., 2017). This combination of confinement and export is important for interpreting aerosol dispersion during boreal summer, including the dispersion of volcanic aerosol. Previous work on the 2011 Nabro eruption debated whether its plume reached the stratosphere directly or was lofted by monsoon ascent. Bourassa et al. (2012) proposed that the plume remained in the upper troposphere and was subsequently transported into the stratosphere by large-scale ascent in the monsoon, whereas later studies showed evidence of direct stratospheric injection, independent of monsoon-driven lifting (e.g., Fromm et al., 2013; Vernier et al., 2013).

Lines 96 You should add a sentence to explain how βair is distinguished from βparticles.

We thank for the Reviewer for this comment and clarify that the COBALD measurement does not directly separate molecular and particle backscatter; it measures their sum. The molecular contribution (β_{air}) is obtained in post-processing by computing the Rayleigh backscatter from the collocated pressure and temperature profiles, and the particle contribution ($\beta_{particles}$) is then derived as the residual after subtracting β_{air} from the measured total backscatter. We have added this clarification in the revised manuscript.

> *The instrument measures only the total backscatter ($\beta_{total} = \beta_{air} + \beta_{particles}$); β_{air} is calculated in post-processing from Rayleigh scattering using the measured pressure and temperature profiles, and $\beta_{particles}$ is obtained as $\beta_{total} - \beta_{air}$.*

Line 165 Please re-word "are empirically highlighted" – I think the criterion is really just that BSR is high without high RH.

Thank you for the suggestion. We agree that "empirically highlighted" was misleading. In the revised manuscript, the highlighted regions are identified using objective threshold criteria rather than subjective highlighting. Specifically, we exclude cirrus using $BSR_{455} > 1.2$, $RH_{ice} > 70\%$, and CI > 7, then define aerosol layers by $BSR_{455} > 1.1$, and finally classify them using CI = 6 (Raikoke plume: CI > 6; ATAL: CI < 6). The text has been revised accordingly.

Line 172 "Typical ATAL profiles … " – do you mean typical enhancements in the profiles?

We reworded "Typical ATAL profiles" to "ATAL-related enhancements in COBALD BSR profiles" to clarify that we refer to the altitude/θ range of ATAL enhancements rather than the full profile.

> *In general, ATAL-related enhancements in COBALD BSR_{455} profiles are largely confined to 360 to 400 K, with a core near 370 to 390 K. Occasional extensions up to 420 to 440 K occur depending on region and year (Vernier et al., 2015, 2018; Appel et al., 2022). The 2013 ATAL profile shown in Fig. 3a is taken from the COBALD measurements over Lhasa reported by Vernier et al. (2015). The 2019 median peak occurs near 417 K, about 33 K above the 2013 ATAL peak at 384 K, corresponding to roughly 1.7 km in altitude in the UTLS based on the 30 July 2019 background sounding. Because the vertical extent of ATAL enhancements varies across regions and years, we emphasize peak magnitude as the more robust difference. The 2019 Raikoke-related median BSR_{455} reaches about 1.25, exceeding the 2013 ATAL peak of about 1.10 (Fig. 3a).*

Lines 172-175 It seems to me that the distinguishing feature of the 2019 profiles is the magnitude of the peak rather than the height. You say the ATAL profile can reach 420-440 K at times.

We agree and revised the text to emphasize peak magnitude as the primary difference (2019 median $BSR_{455} \approx 1.25$ vs 2013 ≈ 1.10), while treating the higher peak altitude (417 K vs 384 K; ~1.7 km) as supporting information given the variability in the ATAL vertical extent.

Figure 3 the thin gray lines are very hard to see – I couldn't see them at all on my screen until I zoomed to at least 300%.

Thank you for pointing this out. We have revised Fig. 3 of our manuscript (Figure 3 in this reply) and increased the visibility of these lines by using a darker gray color and a larger line width.

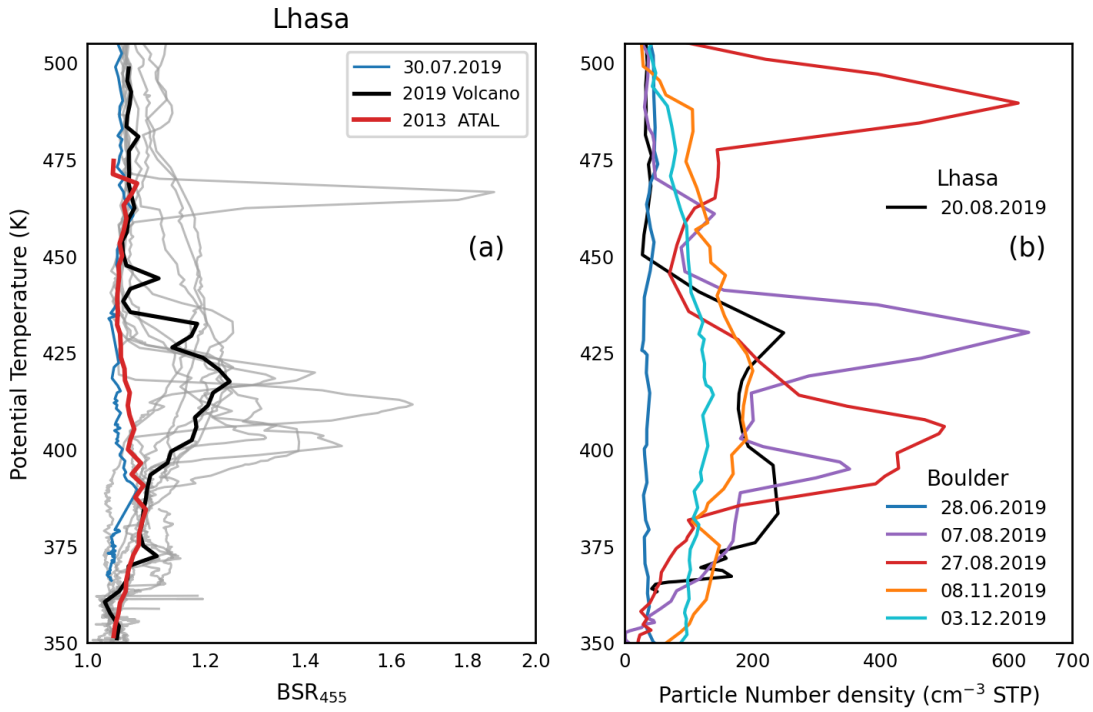

Figure 3 (also Figure 3 in the revised manuscript). (a) COBALD measurements in Lhasa. The black line represents the median BSR_{455} for the 2019 profiles influenced by the volcanic event, and the gray lines show the corresponding individual profiles. The red line shows the median BSR_{455} during the ATAL in 2013. The blue line corresponds to the BSR_{455} on 30 July 2019, which was not affected by the Raikoke eruption. (b) POPS measurements in Boulder and Lhasa.

Lines 184-185 Please re-word "we performed backward-trajectory analyses based on in-situ ballon-borne measurements …" This reads to me that the back trajectories are using data from the balloon measurements.

We rephrased this sentence to clarify that the trajectories are calculated from ERA5 wind fields. The balloon observations are used only to define the trajectory initialization times and potential temperature ranges of the observed plume layer, with parcels released along the balloon flight track.

~~*To verify that the enhanced aerosol layer observed over Lhasa originated from the Raikoke eruption, we performed backward- trajectory analyses based on in-situ balloon-borne measurements over Lhasa, driven by high-resolution ERA5 data (Fig. 4).*~~ *To verify that the enhanced aerosol layers observed over Lhasa are linked to the Raikoke eruption, we calculated ERA5-driven diabatic backward trajectories with CLaMS (Fig. 4). Trajectories were released every second along each balloon ascent within the selected plume-layer potential-temperature intervals indicated by the orange shading in Fig. 2, using iMet-derived time and location (longitude, latitude, pressure, and temperature) as initial conditions. All trajectories were calculated backward to a single common reference time, 21 June 2019 at 18:00 UTC, which serves as the common trajectory endpoint for all cases.*

Lines 184-221 The back trajectories are run for periods from 1.5 to 5 months. Do you have any confidence that the results are meaningful over such a long period of time?

We agree that confidence in backward-trajectory reconstructions decreases as the period becomes longer, even when using high-resolution ERA5-driven CLaMS trajectories. For this reason, we do not include backward trajectories for the September–November flights in the manuscript, since they require tracing air parcels much further back in time. We focus the trajectory analysis on the July–August period, when plume structures remain more coherent and the trajectories provide clearer transport pathway information.

Figure 4 Are the labels on the x-axes date and month? (dd.mm ?)

Yes, these are dates in dd.mm format. We updated the x-axis title to "Date (dd.mm.yy)" in Figure 4 of the revised manuscript (Figure 4 of this reply)

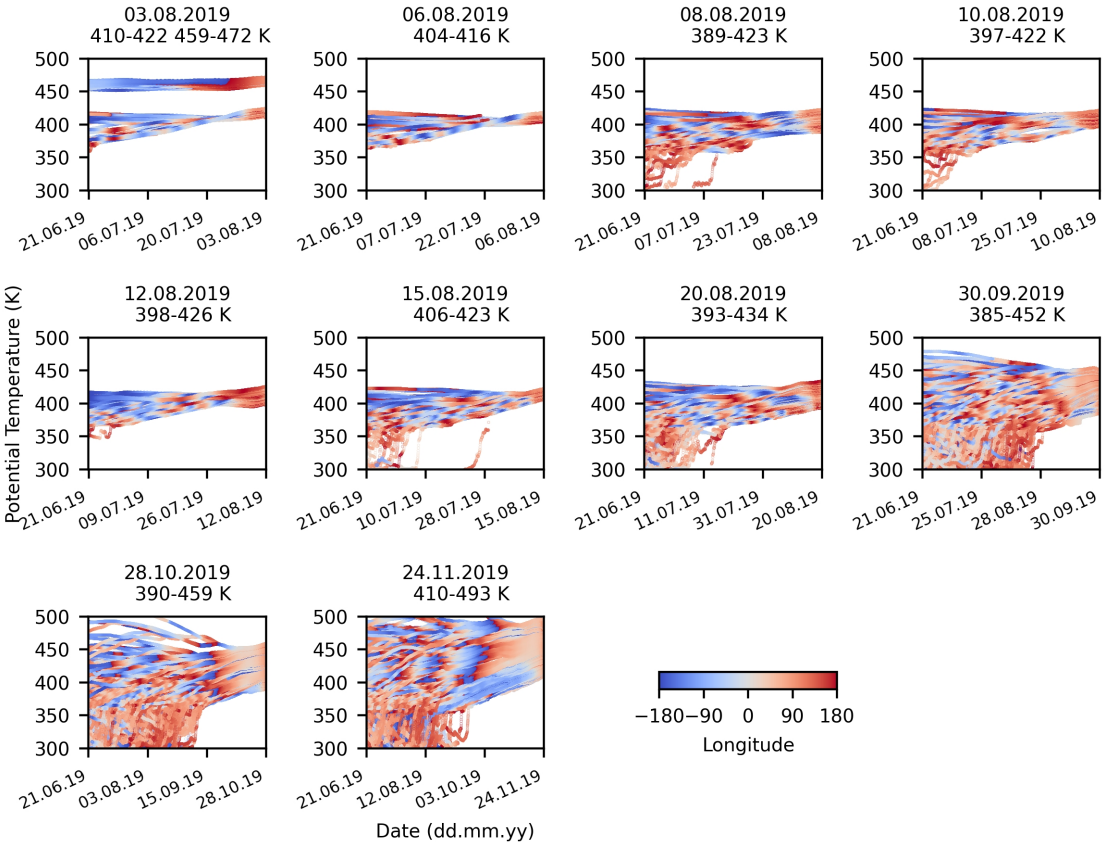

Figure 4 (also Figure 4 in the revised manuscript). Backward trajectories initialized from the Lhasa balloon observations and traced back to the Raikoke eruption reference time (21 June 2019, 18:00 UTC). Only trajectories initialized within the enhanced BSR_{455} potential-temperature range (orange shading in Fig. 2) are shown. Colors indicate trajectory longitude. The x-axis shows date (dd.mm.yy) along the backward integration (right: balloon initialization time; left: eruption reference time).

Figure 4 It would be very helpful to mark the height of the tropopause on these plots.

Thank you for the suggestion. We agree that indicating the tropopause can help interpretation. However, the trajectories in Fig. 4 span a wide range of latitudes across the Northern Hemisphere, and the tropopause potential temperature varies strongly with latitude. Therefore, plotting a single "tropopause line" on each panel would not be representative.

Lines 203-206 I don't quite understand this – what is the denominator of the fraction exactly? You need to give more detail on how you initialized the starting positions and times of the back trajectories., and how many you ran for each date.

Thank you for pointing this out. In Fig. 5, the fraction is defined as (number of trajectories that meet the eruption-region criterion) / (total number of backward trajectories initialized for the corresponding flight date and θ-layer shown in Fig. 4). A trajectory is counted as meeting the criterion if it passes through the eruption-region filter, defined by the TROPOMI-observed SO_2 plume area during the satellite overpass window (24 Jun 2019 22:46–25 Jun 2019 03:50 UTC), at least once.

Backward trajectories are initialized from the selected plume layer(s) for each flight day, using the corresponding starting positions and times measured by the balloon-borne measurement. The denominator is therefore the number of trajectories whose starting θ lies within the selected θ interval(s). For the six cases shown in Fig. 5, the total numbers are 79 and 50 (03 Aug, two θ-layers), 72 (06 Aug), 190 (08 Aug), 165 (10 Aug), and 105 (12 Aug). The corresponding fractions are 5.06%, 6.0%, 9.72%, 3.16%, 6.67%, and 5.71%, respectively. We have added this definition and the per-case trajectory counts to the revised manuscript.

> *In Fig. 5, the reported fraction is ~~the percentage of the total backward trajectories in Fig. 4 that pass through the eruption-region mask during that window. Because this filtering criterion is highly selective, only a small fraction of trajectories remain, and the fractions can be regarded as conservative estimates.~~ defined as (number of trajectories that meet the eruption-region criterion) / (total number of backward trajectories initialized for the corresponding flight date and θ-layer shown in Fig. 4). For the six cases shown in Fig. 5, the total numbers of initialized trajectories are 79 and 50 (03 Aug, two θ-layers), 72 (06 Aug), 190 (08 Aug), 165 (10 Aug), and 105 (12 Aug). Because this filtering criterion is highly selective, only a small fraction of trajectories remains, and the resulting fractions can be regarded as conservative estimates.*

Lines 209-211 Looking at the top right panel of Figure 5 it looks like the air parcel travels directly from the area of Raikoke westwards to Lhasa. However the text says it circles the globe three times, while the red and blue colors of figure 4 (second panel) make it look to me as if the plume circled the globe once.
Could you clarify this point please?

Thank you for pointing this out. The phrase "encircled the globe three times" referred to the satellite-tracked evolution of the VVP core reported by Gorkavyi et al. (2021) and Khaykin et al. (2022), and was not meant to imply that three full revolutions are visible from our single map panel. To avoid confusion, we have removed this wording from the revised manuscript. Figure 5 shows backward trajectories that are consistent with the early stage of the VVP pathway around late July. We have clarified this wording in the revised manuscript.

> *Satellite observations from TROPOMI on Sentinel-5P indicate that the VVP core was entrained into the summertime easterlies around 20–25 July (Gorkavyi et al., 2021; Khaykin et al., 2022). The backward trajectories initialized in the 3 August 2019 plume layer (459–472 K) shown in Fig. 5 are consistent with the late-July stage of this satellite-tracked pathway. The potential temperature of the VVP during its transit through the ASMA, inferred from satellite detections, also closely matches the altitudes of enhanced BSR_{455} (Gorkavyi et al., 2021; Khaykin et al., 2022).*

Lines 219-221 The 'clockwise advection' within AMSA isn't very noticeable to me on the back trajectory plots in Figure 5.

Thank you for the comment. We agree that a clear clockwise rotation is not identifiable from the trajectories as plotted in Fig. 5. We therefore revised the text and removed the wording "clockwise advection", replacing it with a more neutral statement that the trajectories enter and remain within the ASMA region, which is consistent with subsequent transport shaped by the ASMA circulation.

> *From 6 to 20 August 2019, the overall transport pattern remained similar to that on 6 August—corresponding to the main volcanic aerosol plume primarily driven by the subtropical westerly jet. ~~However, after entering the ASMA, some air parcels took different paths: they were advected clockwise within the ASMA's anticyclonic circulation. This clockwise advection diluted the aerosol concentration, contributing to the observed decrease in BSR455.~~ After entering the ASMA, some air parcels deviate from the jet pathway and circulate within the anticyclonic region. This increased spreading of trajectories suggests dispersion and lateral mixing with surrounding air, which may contribute to the observed decrease in BSR_{455}.*

Lines 262-265 It was disappointing to me to read that the upper peaks from 1 August and 3 August were not going to be simulated. Could you perhaps add another sentence to explain why these weren't included too.

Thank you for the comment. The reason why the upper peaks (1 and 3 August) are not simulated is discussed in detail in our response to the major comment (see above). We have added a short reference sentence in the manuscript.

> *In Fig. 7, the SO_2-based tracers are also released at 400–420 K. This setup primarily samples the diluted main plume rather than the higher-altitude trailing filament of the vorticized volcanic plume (VVP). Accordingly, the higher-altitude peak on 3 August 2019 likely originates from the VVP filament near 460–490 K and is not resolved by the 400–420 K release. A sensitivity simulation targeting the upper-level VVP filament shows enhanced tracer fractions near the observation region (not shown here); however, with the currently used CLaMS resolution, this thin and sharp aerosol peak at a single profile location is difficult to reproduce.*

Figure 7 The correlation coefficient seems a limited metric because in some cases the peak is dispersed over a wide altitude range (in other words, you're correlating one gentle curve with another gentle curve, in which situation correlation is not very helpful). Is the relation between tracer fraction and BSR linear across all the different profiles? It looks like it is. Would it be more meaningful to calculate the fit across all the different profiles?

We thank the referee for the insightful comment. The suggested single overall linear fit across all profiles would mainly address amplitude scaling, whereas Fig. 7 is intended to evaluate the vertical structure (shape and peak height) for each individual profile. Because BSR amplitude is not expected to follow one universal linear scaling with a transport tracer across different days, we keep r (after normalization) together with $|\Delta\theta|$ and clarified this point in the manuscript.

Line 323 I think this is the first time you have discussed horizontal entrainment, the previous discussion was about upwelling air diluting the aerosol concentration.

Thank you for this comment. By "horizontal entrainment" we refer to the situation after the trajectories enter the ASMA (from 6 August onward in Fig. 5), where some air parcels circulate within the anticyclonic region and the trajectories spread out. This increased spreading suggests enhanced dispersion and lateral mixing with surrounding air, which may contribute to the observed decrease in BSR_{455}. We have clarified this interpretation in the corresponding discussion paragraph and revised the conclusion accordingly, using the same wording ("dispersion and lateral mixing with surrounding air") rather than introducing "horizontal entrainment" as a new mechanism there.

After entering the ASMA, ~~both upwelling from lower potential temperature levels and horizontal entrainment of surrounding air contribute to this dilution.~~ dilution may be driven by upwelling from lower potential temperature levels and by dispersion and lateral mixing with surrounding air.

Lines 335-337 How have you shown that?

We agree that the original wording was too strong. Our results do not demonstrate global dispersal by the ASMA. Instead, they show that only a small fraction of the Raikoke plume is entrained into the ASMA. Within the ASMA, confinement and summertime diabatic uplift can promote redistribution and dilution in the UTLS and can potentially transport this fraction to higher altitudes, consistent with established ASMA dynamics (e.g., Vogel et al., 2019). We revised the text accordingly.

> *~~In particular, our findings show that the ASMA may play an important role in dispersing aerosols from mid-latitude volcanic injections throughout the global stratosphere.~~ Our results suggest that a small fraction of the Raikoke plume becomes entrained into the ASMA. Within the ASMA, confinement and summertime diabatic uplift can potentially transport these plume fractions to higher altitudes(e.g., Vogel et al., 2019).*

Review of "Transport of volcanic aerosol from the Raikoke eruption in 2019 through the Northern Hemisphere" by Zhen Yang et al. (egusphere-2025-4842)

Original referee comments are in blue.

Our responses are in black with regular bold format. Text from the updated manuscript:

Appears in italic and with 0.5 cm indentation and with the modified parts in red.

General comments

Yang et al. investigate the transport pathways of the volcanic plume emitted by the Raikoke eruption in 2019, with focus on the Asian summer monsoon anticyclone (ASMA) region. The analysis is based on a combination of aerosol backscatter measurements by COBALD sondes flown in Lhasa (China) and model simulations using the CLaMS model. Two types of simulations are presented: backward trajectories, aimed to trace back the observed aerosol plumes to the Raikoke eruption, and global tracer simulations, investigating transport in the model and its sensitivity to different parameters. Aerosol number density profiles from POPS sondes flown in Boulder (USA) are also used to evaluate the results of the tracer simulations.

The paper is well written and fits well the scope of ACP. The observational data are of high quality and nicely combined with the model simulations, including the use of TROPOMI SO_2 satellite retrievals to define the initial state of the eruption. The results are presented clearly and concisely, although some of the assumptions made would require in my opinion further elaboration. The figures are excellent.

I support the publication of the paper. However, I have some comments that I think should be addressed to improve and/or clarify a few aspects of the study, mainly related to the backward trajectory analysis and the use of COBALD data to define the volcanic plume, as well as the overall impact of the paper.

We sincerely thank the reviewers for their encouraging comments and comprehensive revision suggestions, which have significantly enhanced the quality of the manuscript.

1. The "empirical" definition of the regions of enhanced BSR_{455} attributed to the Raikoke eruption (orange shadings in Fig. 2), which are used to initialize the backward trajectories, requires some clarification. I generally agree with the identified regions, but I think the criteria used for their classification should be discussed in more detail and could be at least partly quantified.

The main issue is the separation of the volcanic signal from aerosol features related to ATAL. There are enhanced BSR_{455} features in the profiles shown in Fig. 2 that are not classified as volcanic plume, likely because they are related to ATAL, but no explanation is given on why these regions are not considered. For example, on 10-08-2019, an enhanced BSR455 layer starts at ~140 hPa, well below the marked onset of the volcanic plume (84 hPa). Other small features can be seen on 01-08-2019 (~80-130 hPa), 06-08-2019 (~120-140 hPa), and 12-08-2019 (~120-140 hPa). If my interpretation is correct and these features are related to ATAL, I would suggest to discuss this in the text and to highlight them accordingly in Fig. 2 (e.g., by a different color shading). If not, why are these regions excluded?

Secondly, the visual identification of the plume boundaries becomes difficult when the BSR_{455} gradient is smooth, as in the last three flights (Sept-Nov). Here, I have the impression that the lower boundary of the plume does not match the onset of the BSR_{455} enhancement (roughly at 100 hPa), but rather some given threshold in BSR_{455}. Is there a reason to define the lower boundary this way?

One possibility to quantify these criteria could be the use of the COBALD color index (CI), defined as the ratio of the 940-to-455 nm aerosol BSR (i.e., BSR – 1). Using information from both wavelengths, the CI is a proxy of particle size that was used in several studies to separate clouds from aerosols (e.g., Vernier et al., 2015; Brunamonti et al., 2018; Hanumanthu et al., 2020). Here, the CI might help to distinguish the volcanic plume from ATAL, assuming they have different size distributions, and to define its boundaries more accurately. Have you considered looking into this?

We thank the referee for this helpful suggestion. Distinguishing Raikoke aerosol from ATAL using in situ backscatter profiles alone is challenging, because humidity alone cannot distinguish volcanic aerosol from ATAL, and depolarization data are not available for these COBALD measurements. Our revised approach therefore combines BSR, RH_{ice} and CI, and we note that the CI based separation should be regarded as supportive rather than definitive. In the revision, we clarify and partly quantify how the Raikoke related layers (orange shading in Fig. 1 of this reply) were selected for initializing the backward trajectories, and how we separate them from ATAL related enhancements.

We now apply a consistent set of thresholds for the classification. First, we exclude cirrus using $BSR_{455} > 1.2$, $RH_{ice} > 70\%$, and $CI > 7$. In the remaining cloud free parts, aerosol layers are identified using a uniform threshold of $BSR_{455} > 1.1$. When multiple BSR_{455} enhanced layers occur in the same profile, we use the COBALD color index as an additional indicator, applying $CI > 6$, to support the separation between the upper Raikoke layer and lower layers that are more consistent with ATAL.

We also clarify that CI is not used as a stand alone boundary definition. In very clean air where BSR values approach 1, CI can become unstable because it is computed from (BSR−1) at two wavelengths, and it can also be sensitive to small baseline or calibration offsets. We therefore evaluate CI only within BSR_{455} enhanced, cloud free layers and interpret it as a supporting indicator.

These updates are reflected in the Fig. 1 of this reply, where ATAL like enhancements are now highlighted separately from the Raikoke plume. In addition, we provide a supplementary plot (Fig. 2 of this reply) showing box plots of BSR_{455} and CI for the two categories, which supports the separation.

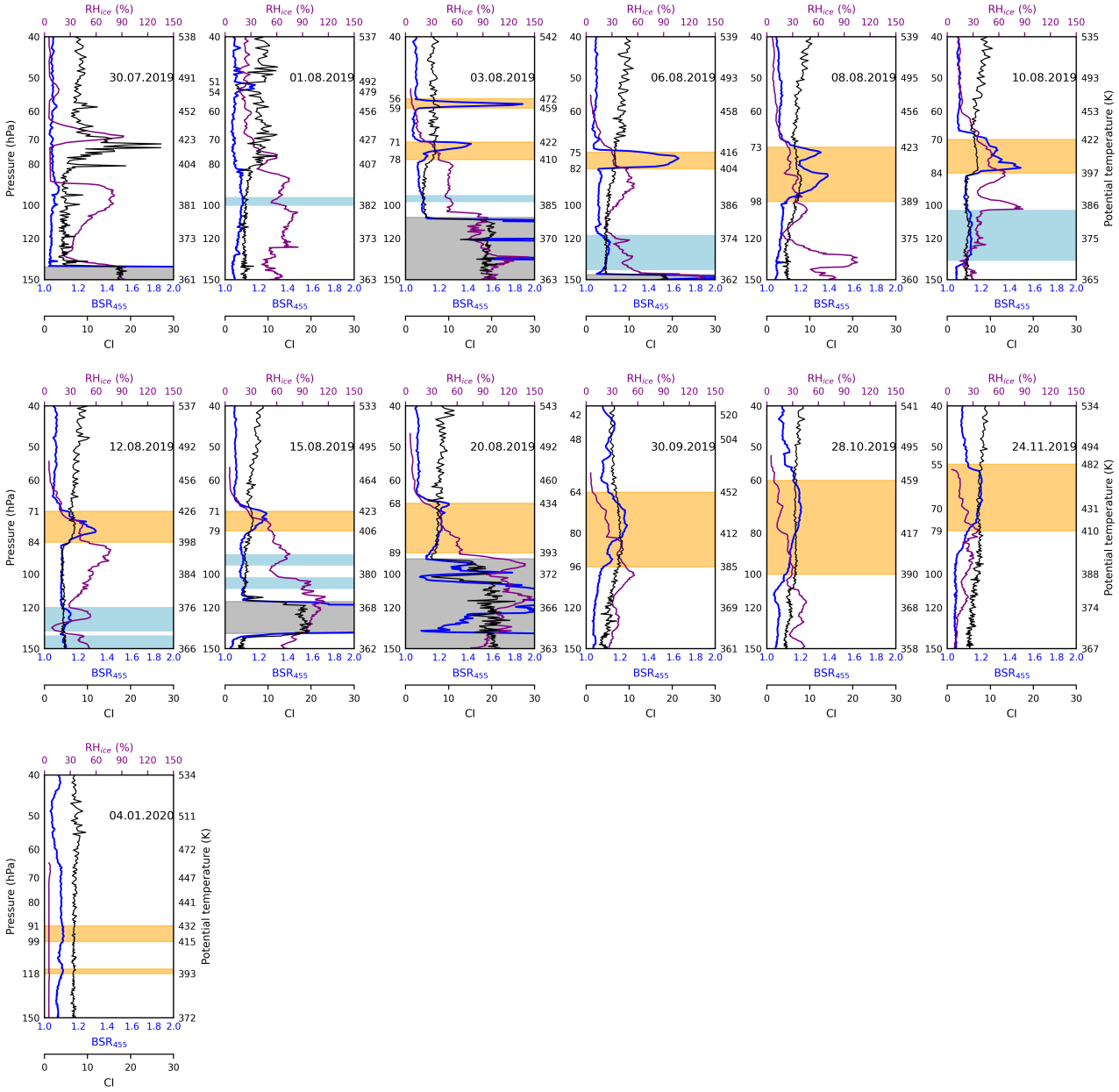

Figure 1 (Figure 2 of the revised manuscript). COBALD and CFH profiles above Lhasa from 30 July 2019 to 4 January 2020. COBALD backscatter ratio at 455 nm (BSR_{455}, blue) and COBALD color index (CI, black) are shown together with CFH relative humidity over ice (RH_{ice}, magenta). Pressure is shown on the left axis and the corresponding potential temperature on the right axis. Orange shading marks the Raikoke-influenced aerosol layers used to initialize the backward trajectories. Light blue shading indicates lower-altitude aerosol enhancements attributed to the ATAL that are not used for plume initialization. Gray shading indicates cirrus conditions.

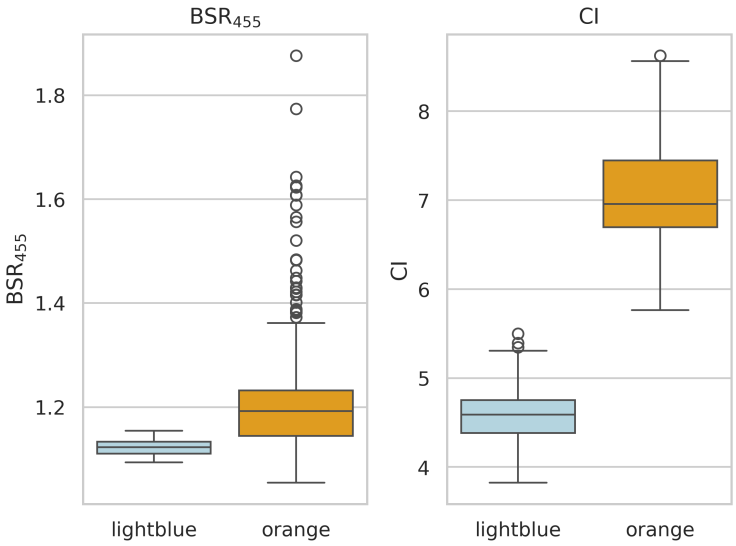

Figure 2. Box plot summary of COBALD BSR_{455} and color index (CI) values sampled within cloud free aerosol layers (BSR_{455} > 1.1) classified as ATAL type (light blue shading in Fig. 1) and Raikoke plume (orange shading in Fig. 1). Boxes show the median and the middle 50% of the data. The whiskers show the typical range, and the circles show unusual values.

2. Since the Boulder profiles are not included in the backward trajectory analysis, the paper focuses almost entirely on transport of the volcanic plume in the ASMA region, rather than the whole Northern Hemisphere (as hinted by the title). The Boulder data are only used to evaluate the results of the tracer simulations, and although the agreement with the model is remarkable (Fig. 8), the discussion of these measurements remains very limited (a few lines on pages 7 and 14). At the same time, the tracer distribution map in Fig. 6 shows that the filament advected over Lhasa represents only a small fraction of the volcanic plume, while most of it stays outside of the ASMA. Therefore, I find that the general discussion is not properly balanced in this respect. I would suggest to try better integrating the Boulder data into the "storyline" of the paper, for example, by adding backward trajectories initialized from these flights into Fig. 5 (or an additional figure). This would allow to frame the entire transport pathway analysis in a more general context, and would be in my opinion a great addition to the paper. Otherwise, it should be at least pointed out more clearly that the ASMA pathway only accounts for a minor fraction of the entire volcanic plume emitted by the Raikoke eruption.

We thank the referee for this insightful comment. We have revised the manuscript according to the reviewer's advice.

To maintain consistent identification of volcanic plumes throughout this paper, we initialize trajectories at the potential temperature interval where the in-situ particle number density exceeds 150 cm^{-3}. This criterion captures the main volcanic plume signal.

Specifically, we now include backward trajectories for the plume layers observed on 7 August 2019 (373–442 K), 27 August 2019 (385–429 K and 480–505 K) in Figure 3 of this reply, and we add the corresponding global three-dimensional tracer simulations for these days on the American continent in Figure 4 of this reply. These additions provide a broader hemispheric context for the transport pathways and clarify how the ASMA-related transport compares with pathways outside the ASMA.

In addition, we revised the discussion to clarify the evolving role of the ASMA in the three-dimensional tracer distributions: during August, during the peak ASMA season, only a minor fraction of the Raikoke tracer is located inside the ASMA, while the majority remains outside; by September, the tracer has become substantially mixed and the difference between the ASMA and non-ASMA regions in the regional distribution is no longer clearly evident.

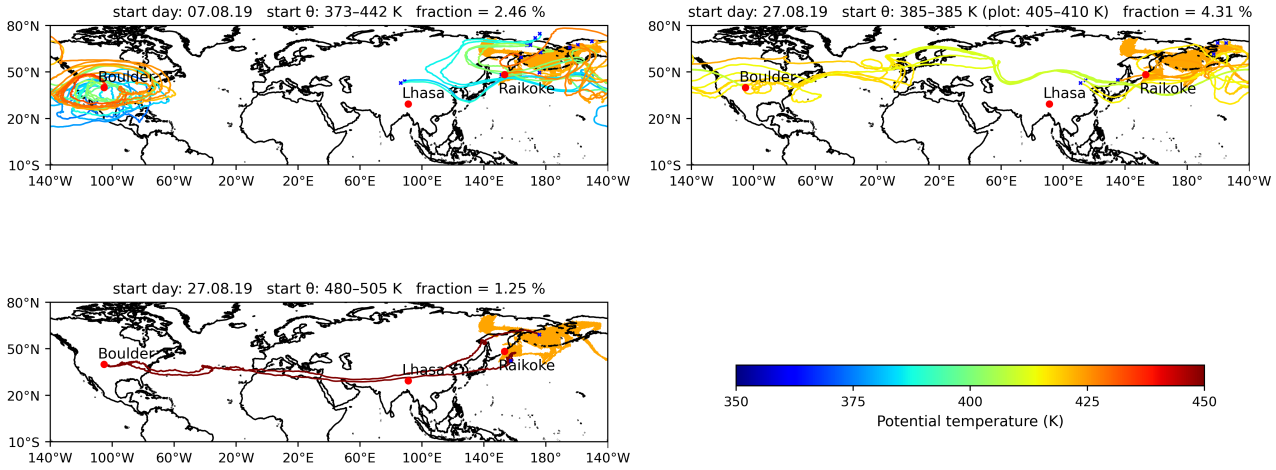

Figure 3 (Figure 6 of the revised manuscript). Backward trajectories for the Boulder flights (7 and 27 August 2019). Only trajectories that intersect the TROPOMI SO_2 mask during 24 June 2019, 22:46 to 25 June 2019, 03:50 UTC are shown. Trajectories are coloured by potential temperature, and the SO_2 mask is shaded in orange. Panel titles give the start day, start θ range, and the fraction of trajectories that satisfy the SO_2 mask criterion. For the 7 August 2019 back trajectories, the fraction is computed for 385 to 429 K, while the plotted trajectories are restricted to 405 to 410 K to better illustrate the transport pathway. Locations of Boulder, Lhasa, and Raikoke are marked.

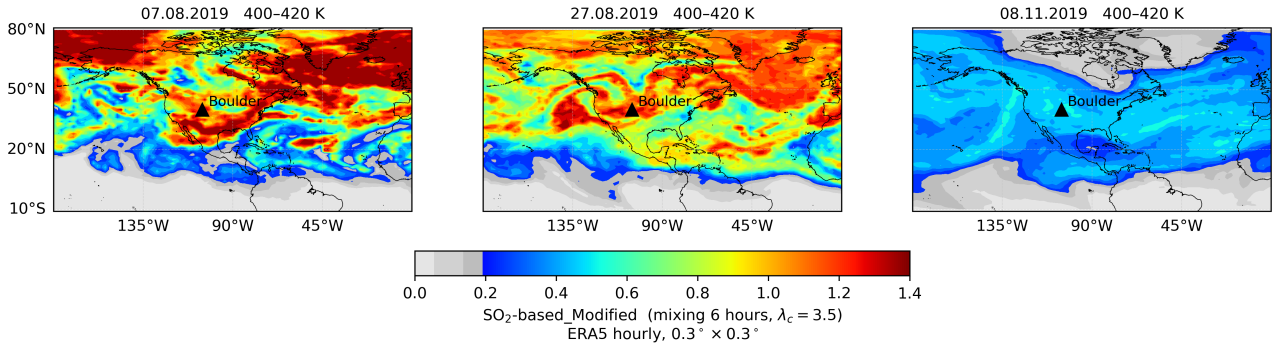

Figure 4 (Figure 8 of the revised manuscript). SO_2-based tracer fractions within the 400–420 K layer over the American sector. The black triangle indicates the location of Boulder.

Specific comments

Page 1, line 15: this sentence requires more context (what does "additional" uplift refer to?).

We removed the statement from the abstract and addressed it consistently regarding comments on pages 16, lines 304–309 (see response below).

Page 2, line 32: consider omitting the definition of VEI (not relevant to this study).

We removed the definition and discussion of the Volcanic Explosivity Index (VEI). We retain the "eruption magnitude" factor but describe it more directly in terms of SO_2 and ash release, and add a brief note on submarine eruptions (e.g. Hunga Tonga 2022).

Several key factors govern the climate impact of volcanic aerosols from an eruption: (1) eruption magnitude; (2) injection height and self-lofting; (3) eruption latitude; and (4) dynamical evolution. ~~*(1) The Volcanic Explosivity Index (VEI) serves as a proxy for eruption intensity (Newhall and Self, 1982), and events with VEI ≥ 4 can inject vast quantities of SO_2, water vapor, and ash, causing marked climate perturbations.*~~ *Eruption magnitude can be characterized by the amount of SO_2 and ash released, which largely controls aerosol formation potential and radiative forcing. Notably, substantial perturbations of stratospheric water vapour and aerosol microphysics have also been reported for the 2022 Hunga Tonga eruption despite modest SO2 injection (Carn et al., 2022; Zhu et al., 2022). (2) Eruption products injected directly into the stratosphere, as well as volcanic plumes in the upper troposphere that self-loft into the lower stratosphere through radiative heating, can persist much longer than plumes confined to the troposphere (Toohey et al., 2025). (3) Aerosols from tropical eruptions are transported most efficiently via the Brewer–Dobson circulation (Brewer, 1949; Dobson, 1956; Butchart, 2014), whereas mid-latitude eruption aerosols can still reach the tropics through Rossby-wave breaking or transport by the Asian Summer Monsoon Anticyclone (ASMA) (Konopka et al., 2009; Kloss et al., 2021; Wu et al., 2023). (4) UTLS jet streams, cyclones, anticyclones, and the stratospheric circulation govern dispersion patterns and dilution rates.*

Page 2, line 44: add some references for the chemical trapping in the ASMA, e.g. Park et al. (2007), Randel et al., (2010) (see reference list below).

Yes, the relevant references have been added.

Deep convection injects pollutants into the UTLS, where the ASMA's strong anticyclonic circulation acts as a dynamical transport barrier, confining these air masses over Asia during ascent into the stratosphere (e.g., Park et al., 2007; Randel et al., 2010; Fadnavis et al., 2014; Santee et al., 2017; Vogel et al., 2019).

Park, M., Randel, W. J., Gettleman, A., Massie, S. T., and Jiang, J. H.: Transport above the Asian summer monsoon anticyclone inferred from Aura Microwave Limb Sounder tracers, J. Geophys. Res., 112, D16309, https://doi.org/10.1029/2006JD008294, 2007.

Randel, W. J., Park, M., Emmons, L., Kinnison, D., Bernath, P., Walker, K. A., Boone, C., and Pumphrey, H.: Asian Monsoon Transport of Pollution to the Stratosphere, Science, 328, 611–613, https://doi.org/10.1126/science.1182274, 2010.

Fadnavis, S., Schultz, M. G., Semeniuk, K., Mahajan, A. S., Pozzoli, L., Sonbawne, S., Ghude, S. D., Kiefer, M., and Eckert, E.: Trends in peroxyacetyl nitrate (PAN) in the upper troposphere and lower stratosphere over southern Asia during the summer monsoon season: regional impacts, Atmos. Chem. Phys., 14, 12 725–12 743, https://doi.org/10.5194/acp-14-12725-2014, 2014.

Santee, M. L., Manney, G. L., Livesey, N. J., Schwartz, M. J., Neu, J. L., and Read, W. G.: A comprehensive overview of the climatological composition of the Asian summer monsoon

anticyclone based on 10 years of Aura Microwave Limb Sounder measurements, J. Geophys. Res., 122, 5491–5514, https://doi.org/10.1002/2016JD026408, 2017.

Vogel, B., Müller, R., Günther, G., Spang, R., Hanumanthu, S., Li, D., Riese, M., and Stiller, G. P.: Lagrangian simulations of the transport of young air masses to the top of the Asian monsoon anticyclone and into the tropical pipe, Atmos. Chem. Phys., 19, 6007–6034, https://doi.org/10.5194/acp-19-6007-2019, 2019.

Page 3, line 79: which model of iMet radiosonde was used?

We used an International Met Systems (InterMet) iMet-1-RSB radiosonde. We have added the specific radiosonde model in the instrument description.

Balloons were equipped with an electrochemical concentration cell (ECC) ozonesonde, a cryogenic frostpoint hygrometer (CFH), a compact optical backscatter aerosol detector (COBALD), and an International Met Systems (InterMet) iMet-1-RSB radiosonde (GRUAN Lead Centre, 2025). ECC measurements are not analyzed in this study.

GRUAN Lead Centre: InterMet iMet-1 (iMet-1-RSB) — GRUAN instrument information (radiosonde models), https://www.gruan.org/instruments/radiosondes/sonde-models/intermet-imet-1, accessed 13 Jan 2026, 2025.

Page 3, line 80: I suggest adding a table to summarize date, time, location and payload of all analyzed balloon flights, and possibly to introduce a sequential numbering of the flights (e.g. F1, F2, ...).

Site	Flight ID	Date	Mid-ascent time (UTC)	Key instruments	Observed plume layer: θ (K)	Observed plume layer: p (hPa)
Lhasa	F01	30.07.19	17:58	COBALD CFH	–	–
	F02	01.08.19	15:45	COBALD CFH	–	–
	F03	03.08.19	15:23	COBALD CFH	410–422; 459–472	78–71; 59–56
	F04	06.08.19	15:26	COBALD CFH	404–416	82–75
	F05	08.08.19	15:10	COBALD CFH	389–423	98–73
	F06	10.08.19	16:05	COBALD CFH	397–422	84–70
	F07	12.08.19	15:49	COBALD CFH	398–426	84–71
	F08	15.08.19	17:24	COBALD CFH	406–423	79–71
	F09	20.08.19	17:14	COBALD CFH POPS	393–434	89–68
	F10	30.09.19	15:34	COBALD CFH	385–452	96–64
	F11	28.10.19	15:24	COBALD CFH	390–459	100–60
	F12	24.11.19	15:09	COBALD CFH	410–482	79–55
	F13	04.01.20	15:29	COBALD CFH	393–399; 415–432	118–115; 99–91
Boulder	F14	28.06.19	17:05	POPS	–	–
	F15	07.08.19	17:08	POPS	373–442	122–73
	F16	27.08.19	16:38	POPS	385–429; 480–505	117–80; 59–52
	F17	08.11.19	17:58	POPS	389–435	107–76
	F18	03.12.19	18:05	POPS	–	–

Table 1 (Table 1 of the revised manuscript). Summary of analyzed balloon flights at Lhasa and Boulder, including sequential flight ID, date, mid-ascent time (UTC), key instruments used in this study, and the potential temperature (θ) and pressure (p) ranges of the observed volcanic plume layer. The plume layer was identified from COBALD measurements where BSR_{455} > 1.1 and CI > 6, and from POPS measurements where the particle number concentration exceeded 150 cm^{-3}. Mid-ascent time denotes the midpoint of the ascent period from launch to balloon burst. The "Key instruments" column lists only the instruments analyzed in this work; additional payload components were flown but are not listed here. A dash (-) denotes that no volcanic plume layer was identified for that flight.

Page 5, lines 98-100: I cannot find the source of the COBALD uncertainties given here in Vernier et al. (2015), neither the "maximum BSR uncertainties" of 1.3 % at 940 nm and 0.2 % at 455 nm at ground level, nor the 5 % at 940 nm and 1 % at 455 nm at 10 km altitude. How are these numbers obtained? Vernier et al. (2015) only estimate a 5 % uncertainty for the entire profile, due to physical constraints, and 1 % precision in the UTLS, without differentiating between the two channels. The same uncertainty of 5 % is also reported by other studies using COBALD data in the lower troposphere (Brunamonti et al., 2021) and UTLS (Reinares Martínez et al., 2021). Considering that the retrieval algorithm of COBALD BSR involves empirically-determined instrumental parameters as well as the measured temperature and pressure to calculate the molecular extinction profile, I doubt that such high accuracies can be achieved.

We agree that our previously stated "maximum BSR uncertainties" specified separately by wavelength channel and altitude are not supported by Vernier et al. (2015). We have therefore removed these values and revised the text. In the revised manuscript, we adopt the commonly used COBALD uncertainty characterization: an absolute error interval of ~5% for the BSR profile and a precision better than ~1% in the UTLS (Vernier et al., 2015), consistent with other COBALD-based studies (e.g., Brunamonti et al., 2021; Reinares Martínez et al., 2021).

~~*The maximum BSR uncertainty is 1.3 % at 940 nm and 0.2 % at 455 nm at ground level. At 10 km altitude, uncertainties increase to 5 % and 1 % at 940 nm and 455 nm, respectively (Vernier et al., 2015).*~~ *COBALD BSR uncertainty is typically characterized by an absolute error interval of about ~5% for the profile, while the precision is better than ~1% under UTLS conditions (Vernier et al., 2015; Brunamonti et al., 2021; Reinares Martínez et al., 2021).*

Page 5, lines 106-107: I would be more conservative with the CFH uncertainty. Vömel et al. (2016) state that the uncertainty "may be" as low as 2 % in the lower troposphere and 5 % at the tropical tropopause, under good operating conditions of the mirror temperature controller. The mirror temperature controller is the largest source of uncertainty in CFH measurements and oscillations around the real frostpoint can be up to ±0.5 K, corresponding to ±10 % in H2O mixing ratio at UTLS conditions (e.g., see Poltera et al., 2025). Based on Fahey et al. (2014), I think a more realistic estimate of the CFH uncertainty in the stratosphere is ±10 %, unless the performance of the mirror temperature controller is evaluated specifically for each flight.

We revised the manuscript to reflect that the 2 % (lower troposphere) and 5 % (tropical tropopause) values in Vömel et al. (2016) apply only under good operating conditions. Given that the mirror temperature controller can dominate the uncertainty in the UTLS, we now adopt a conservative ±10 % uncertainty for CFH water vapor measurements in the UTLS and

lower stratosphere, consistent with Fahey et al. (2014) and the discussion in Poltera et al. (2025).

> ~~*The measurement uncertainty is approximately 2 % in the lower troposphere and increases to 5 % near the tropical tropopause (Vömel et al., 2016).*~~ *CFH uncertainties may be as low as ~2 % in the lower troposphere and ~5 % near the tropical tropopause under good operating conditions (Vömel et al., 2016). For UTLS conditions we use a conservative uncertainty of ±10 % (Fahey et al., 2014; Poltera et al., 2025).*

Page 6, line 138: is temperature really needed to define the starting positions?

Temperature is not an independent variable to define the starting positions. Since our trajectory analysis is performed in isentropic coordinates, we use potential temperature as the vertical coordinate, which is derived from the measured pressure and temperature. We clarified this in the revised manuscript.

> *Diabatic backward trajectories are initialized every second along the balloon's vertical ascent profile, using the in-situ measurements of temperature (for deriving potential temperature), pressure, time, longitude, and latitude to define the start positions.*

Page 6, line 152: add a short explanation of the physical meaning of the critical Lyapunov exponent. Does a higher λc correspond to more or less mixing?

We added a short explanation of the physical meaning of the critical Lyapunov exponent. In the CLaMS mixing scheme, parameterized mixing is triggered when the integral deformation between neighboring air parcels exceeds the critical value $\gamma_c=\lambda_c \Delta t$, where Δt is the mixing interval. Thus, for a fixed Δt, a larger λ_c (larger γ_c) requires stronger deformation to trigger mixing and corresponds to less frequent parameterized mixing (and vice versa).

> *To assess how different mixing intensities influence the reconstruction of volcanic plume transport processes, two simulations were conducted:*
>
> *(i) a control simulation with mixing every 24 hours and $\lambda_c = 1.5$;*
>
> *(ii) a modified simulation with mixing every 6 hours and $\lambda_c = 3.5$.*
>
> *In the CLaMS mixing scheme, parameterized mixing is triggered when the integral deformation between neighboring air parcels exceeds an empirical critical deformation $\gamma_c = \lambda_c \Delta t$, where λ_c is the critical Lyapunov exponent and Δt is the advective time step (mixing interval). For a given Δt, a larger Δt (thus a larger γ_c) requires stronger deformation to trigger mixing and therefore corresponds to less frequent parameterized mixing (and vice versa) (Konopka et al., 2004, 2007). In our setup, the modified simulation corresponds to enhanced parameterized mixing compared to the control simulation. Throughout most of the paper we show results from the modified simulation, as these agree better with the observations. Sensitivity to parameterized mixing intensity and comparisons with the control simulation are discussed in Sect. 5.1. The mixing configurations and the additional sensitivity runs (rectangular mask and coarser ERA5 input) are summarized in Table 2.*
>
> *Konopka, P., et al., 2004: Mixing and ozone loss in the 1999–2000 Arctic vortex: Simulations with the three-dimensional Chemical Lagrangian Model of the Stratosphere (CLaMS), J. Geophys. Res., 109, D02315, doi:10.1029/2003JD003792.*

Konopka, P., et al., 2007: Contribution of mixing to upward transport across the tropical tropopause layer (TTL), Atmos. Chem. Phys., 7, 3285–3308, doi:10.5194/acp-7-3285-2007.

Page 7, lines 159-160: the cloud-filtering criteria used here (BSR_{455} > 1.2, RH_{ice} > 70 %) are those derived by Yang et al. (2023), which are, to my understanding, a modified version of the criteria used in previous studies (Vernier et al., 2015; Brunamonti et al., 2018; Hanumanthu et al., 2020), without taking the color index (CI) into account. As I already mentioned, the spectral information contained in the CI is crucial to make a physically-based (rather than empirical) discrimination, since it allows to distinguish size effects (change in BSR and CI) from number density effects (change in BSR but no change in CI). Therefore, I think it would be very interesting to investigate the CI here, as this may provide a quantitative basis for a more accurate definition of the volcanic plume and its boundaries.

We agree that CI provides important spectral (particle-size) information. We revised the manuscript and now identify cirrus using a combined criterion (BSR_{455}> 1.2, RH_{ice}> 70%, and CI > 7). Different studies use different threshold combinations and we require all three conditions to be met to classify a data point as cirrus.

Cirrus clouds are identified using a combined criterion of BSR_{455}> 1.2, RH_{ice}> 70% and CI > 7 (Vernier et al., 2015; Brunamonti et al., 2018; Hanumanthu et al., 2020; Yang et al., 2023).

Page 7, line 163: if "coexist" means that an aerosol layer and a cirrus cloud overlap in altitude, then the two signals cannot be distinguished (rather than "it becomes difficult"). If they coexist in the same profile but on different altitude levels, then the visual identification may become more difficult, but the signals can still be isolated quantitatively (e.g., using the CI). Please clarify.
We clarified the meaning of "coexist". If cirrus and aerosols are vertically separated within a profile, the aerosol signal can still be isolated quantitatively (e.g., using BSR and CI); however, if they overlap at the same altitude, the aerosol contribution cannot be reliably separated because the cirrus signal dominates.

~~*When cirrus clouds and aerosols coexist, it becomes difficult to isolate the aerosol signal because cirrus BSR455 values are significantly higher than those of aerosols.*~~ *When cirrus and aerosols occur within the same profile, aerosol and cloud signals can generally be separated if they are vertically distinct (e.g., using BSR and CI), whereas if a cirrus cloud overlaps the aerosol layer at the same altitude, the aerosol contribution cannot be reliably isolated because cirrus BSR_{455} typically dominates. Thus, the aerosol cannot be reliably detected or quantified under such conditions.*

Page 7, line 165: I suggest "determined by visual inspection" instead of "empirically highlighted".

In the revised manuscript, the highlighted regions are identified using threshold criteria. Specifically, we first exclude cirrus using BSR_{455} > 1.2, RH_{ice} > 70%, and CI > 7, then define aerosol layers by BSR_{455} > 1.1, and finally classify them using CI = 6 (Raikoke: CI > 6; ATAL/background: CI < 6). We have revised the text accordingly.

~~*Regions showing enhanced BSR_{455} — most likely due to Raikoke aerosols — are empirically highlighted in orange in Fig. 2.*~~ *Using these criteria, we exclude cirrus-contaminated layers. Remaining enhancements with BSR_{455} > 1.1 are treated as aerosol layers and then classified using a CI threshold of 6: layers attributed to the Raikoke plume (CI > 6) are highlighted in*

orange in Fig. 2, while layers more consistent with ATAL aerosol (CI < 6) are highlighted in light blue. We note that CI is used here as an additional indicator within aerosol layers and should be interpreted with caution, and that the ATAL identification in our dataset is limited. In very clean air where BSR values at both wavelengths approach 1, CI can become unstable; we therefore apply CI only within aerosol layers with BSR_{455} > 1.1 after excluding cirrus.

Page 7, lines 171-172: I presume the ATAL profile from 2013 shown in Fig. 3a is the COBALD profile from Lhasa by Vernier et al. (2015). Is this correct? Please add a citation.
Yes, this is correct. The 2013 ATAL profile shown in Fig. 3a corresponds to the COBALD measurements over Lhasa presented by Vernier et al. (2015). We have added the citation in the manuscript.

The ATAL profile from 2013 shown in Fig. 3a is taken from the COBALD measurements over Lhasa reported by Vernier et al. (2015).

Page 7, line 174: how much does 33 K potential temperature correspond in altitude (roughly)?
Using the θ–altitude relationship from the 30 July 2019 background sounding, a separation of 33 K around the tropopause corresponds to roughly ~1.7 km. We have added this approximate altitude difference to the manuscript.

Page 10, line 199: quantify "extreme" BSR_{455} values.
We quantified "extreme" by reporting the peak and 95th-percentile BSR_{455} within the identified plume layer (orange shading in Fig. 2). Peak BSR_{455} decreases from up to 1.88 in early August (p95 up to 1.77) to ≤ 1.25 during 30 September–24 November (p95 ≤ 1.24).

Over the following three months, as the ASMA weakened seasonally, air from lower potential-temperature levels increasingly influenced the Lhasa profiles. During this period, peak BSR_{455} within the identified plume layer (orange shading in Fig. 2) decreased from values up to 1.88 in early August 2019(95th percentile up to 1.77) to ≤ 1.25 from 30 September to 24 November 2019 (95th percentile ≤ 1.24), indicating progressive dilution of the volcanic aerosol layer by relatively aerosol-poor air from the lower troposphere.

Page 10, lines 204-206: why should the filtering criterion be considered "highly selective"? Is this related to the spatial/temporal extent of the mask, or its "patchiness"? Would it help to use a more compact domain (e.g., the rectangular mask used in Section 4.3), or to extend the considered time window? And what are the source regions of the > 90 % trajectories that are not shown? This is a key point of the paper, so I think some more elaboration is required.

We use the full TROPOMI-observed SO_2 plume footprint during the satellite overpass as the filtering criterion because it represents the actual observed situation. In this sense, Fig. 5 of the revised manuscript provides a conservative estimate: trajectories are selected only if they intersect the observed plume footprint within the overpass time window. This makes the criterion "highly selective" mainly because both the spatial footprint and, in particular, the temporal window are narrow, so only a small fraction of trajectories satisfy the constraint.

To assess the sensitivity to the spatial and temporal definition of the filter, we performed two additional tests. First, we approximate the TROPOMI footprint by a broader rectangular domain (137–215°E, 42–73°N; Fig. 5 of this reply) while keeping the original overpass time window (24 June 2019, 22:46 UTC to 25 June 2019, 03:50 UTC) in Fig. 6 of this reply.

Second, we apply the same rectangular domain but extend the time window to 7 days (21 June 2019, 18:00 UTC to 28 June 2019, 18:00 UTC) in Fig. 7 of this reply. With the original TROPOMI footprint and overpass window, the fractions of trajectories reaching the eruption region are ~3–10% across the analyzed layers/dates, whereas the relaxed rectangular domain and 7 days window criterion increases these fractions to ~12–28%. We interpret the latter range as an upper bound under a looser, yet still reasonable, filter. The remaining trajectories largely represent background transport pathways during the specified time window.

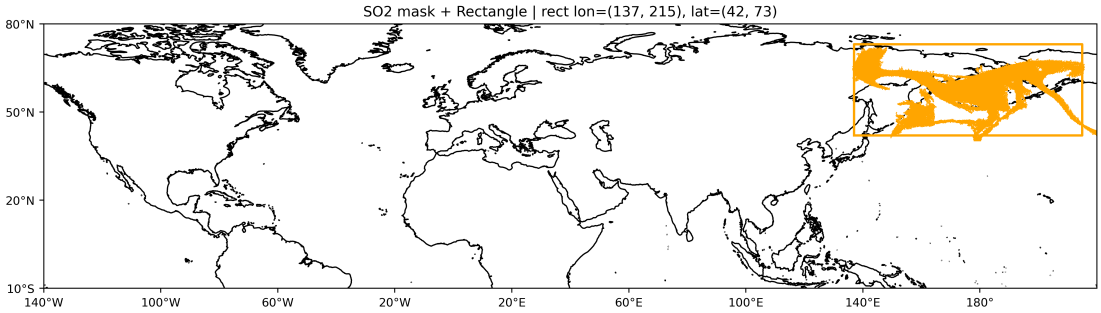

Figure 5. TROPOMI SO_2 plume footprint used for trajectory filtering (orange shading) and its rectangular approximation (137–215°E, 42–73°N; orange box).

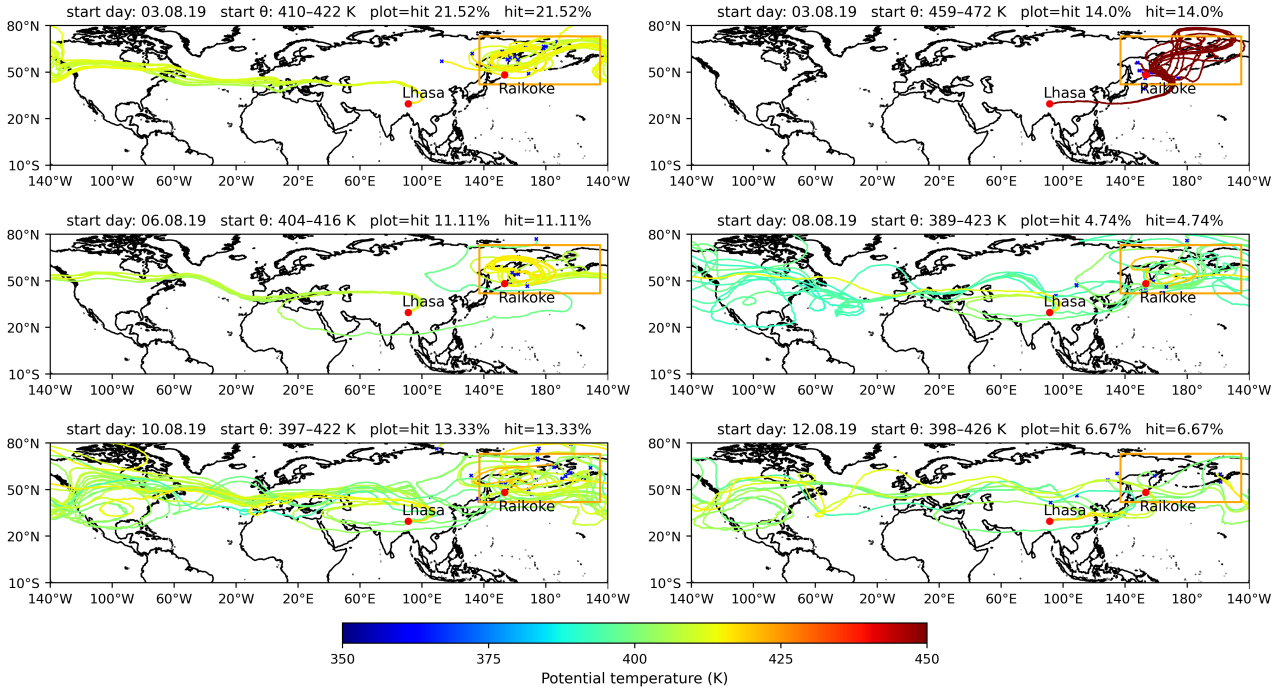

Figure 6. Backward trajectories filtered by intersection with the rectangular domain (137–215°E, 42–73°N) within the original TROPOMI overpass time window (24 Jun 2019, 22:46 UTC–25 Jun 2019, 03:50 UTC).

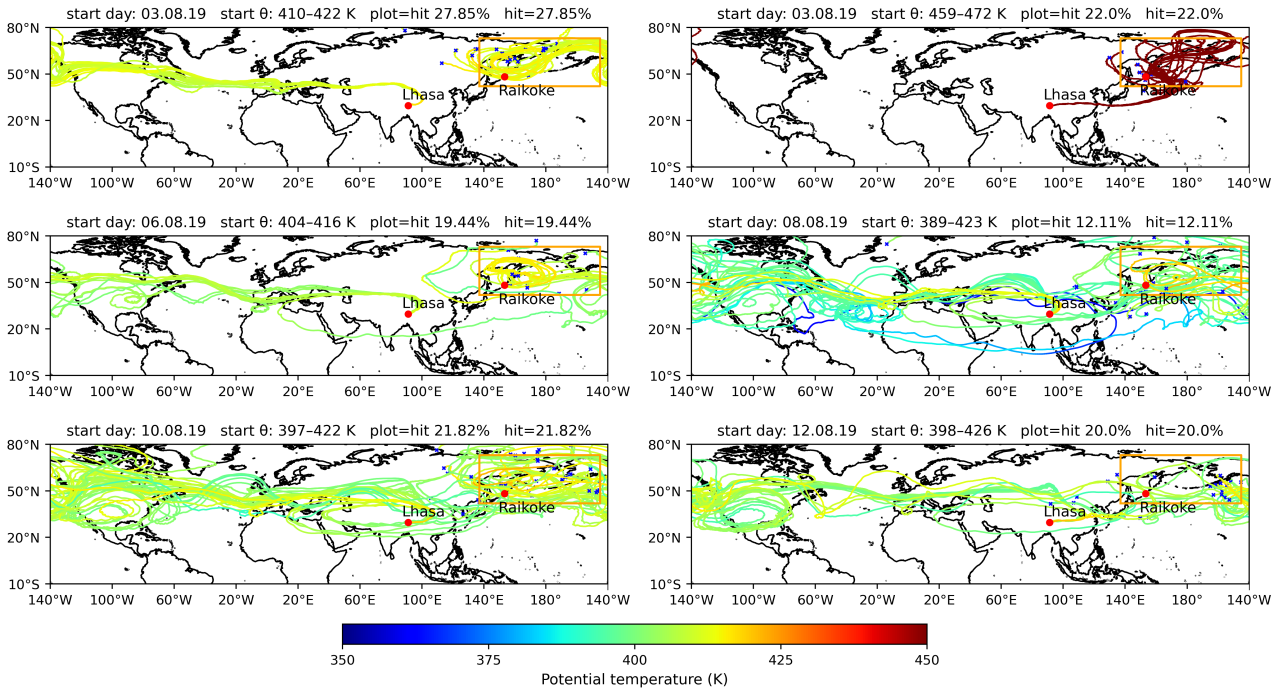

Figure 7. Same as Fig. 6, but using an extended 7-day time window (21 Jun 2019, 18:00 UTC–28 Jun 2019, 18:00 UTC) to test sensitivity to the temporal definition of the filter.

A sensitivity test shows that the fraction of backward trajectories reaching the eruption region is ∼3–10% when using the original TROPOMI SO_2 footprint and satellite-pass time window, but increases to ∼12–28% when applying a broader rectangular domain (137–215° E, 42–73° N) and extending the time window to 7 days. The retained trajectories still follow the same main transport pathways shown here, providing confidence in the identified transport patterns.

Page 10, line 209: which satellite? Is this statement referring to Khaykin et al. (2022)?

We clarified the satellite instrument by TROPOMI on Sentinel-5P and reworded the sentence to specify that the consistency with Fig. 5 refers to the backward trajectories initialized in the 3 August plume layer (459–472 K).

~~*Satellite tracking shows that the primary VVP was entrained in summertime easterlies around 20–25 July, circled the globe three times, and passed south of the Tibetan Plateau on 31 July. This pathway aligns with the backward trajectories in Fig. 5. Furthermore, the potential temperature measured by the satellite during its ASMA transit also closely matched the altitudes of enhanced BSR455 (Gorkavyi et al., 2021; Khaykin et al., 2022).*~~ *Satellite observations from TROPOMI on Sentinel-5P indicate that the VVP core was entrained into the summertime easterlies around 20–25 July (Gorkavyi et al., 2021; Khaykin et al., 2022). The backward trajectories initialized in the 3 August 2019 plume layer (459–472 K) in Fig. 5 are consistent with the late-July phase of this satellite-tracked pathway. The potential temperature of the VVP during its transit through the ASMA inferred from satellite detections also closely matches the altitudes of enhanced BSR_{455} (Gorkavyi et al., 2021; Khaykin et al., 2022).*

Page 11, lines 218-221: why are the backward trajectories of the September-November flights not included?

We did not include backward trajectories for the September–November flights (also the backward trajectories for Boulder on 8 November 2019) because they require tracing the air

parcels much further back in time. Although we have adopted the high-resolution ERA5 data as the input data, the reliability of trajectory reconstruction inevitably decreases over time. In addition, by September–November the Raikoke plume is substantially diluted and more thoroughly mixed with background air, so coherent pathway information becomes less distinct. We therefore focus the trajectory analysis on the July–August period, when plume structures are still relatively coherent and the trajectories provide clearer transport-pathway information.

Page 12, line 248: I suggest adding a table to summarize the different model runs and their main characteristics (mixing parameters, injection region/height, etc.). I would also recommend introducing a more compact notation for these simulations (e.g., "SO2-based_control" → CTRLSO2), and perhaps a more meaningful name for the "modified" scenario (e.g. "mixing-enhanced", "MIX-ENH" or similar).

Thank you for the suggestion. We added a new table (Table 2 in the manuscript) summarizing the model runs and their key settings (injection region/layers, mixing interval, and the critical Lyapunov exponent λc). We still retained the original descriptive simulation names (SO_2-based_Control, SO_2-based_Modified, and rectangle-based_Modified), because they are more informative and allow readers to infer the main differences directly from the naming.

Simulation	Injection region	Injection layer	Mixing interval	λ_c	Notes
All simulations listed below are driven by ERA5 at $0.3^\circ \times 0.3^\circ$ *spatial and 1 hour temporal resolution. Figure A2 shows the* SO_2*-based_Control simulation repeated with coarser ERA5 input (*$1^\circ \times 1^\circ$ *spatial, 6 hours temporal resolution).*					
SO_2-based_Control	satellite SO_2 plume mask	380–400 K; 400–420 K; 420–440 K	24 hours	1.5	reference run
SO_2-based_Modified	satellite SO_2 plume mask	380–400 K; 400–420 K; 420–440 K	6 hours	3.5	main run; best agreement with observations
rectangle-based_Modified	(163°E–170°W, 49°N–62°N)	380–400 K; 400–420 K; 420–440 K	6 hours	3.5	sensitivity to injection-region definition

Table 2 (Table 2 of the revised manuscript). Summary of tracer simulations using different injection-region definitions (satellite SO_2 plume mask and a rectangular domain), including injection layer, mixing interval, and critical Lyapunov exponent (λc).

Page 12, lines 250-252: any idea why is the tracer distribution in the control run more fragmented?

The more fragmented tracer distribution in the control run mainly reflects the different mixing settings: in CLaMS, parameterized mixing is triggered when the integrated deformation exceeds γc=λc Δt, and γc is larger in the control run than in the modified run, so mixing is activated less often and in larger, discrete steps, yielding a patchier and more fragmented tracer field.

Page 13, line 259: the quantity "BSR – 1" is usually termed "aerosol BSR" (ABSR: Cirisan et al., 2014) or particle BSR (PBSR: Reinares Martínez et al., 2021), as it represents the ratio of aerosol-

to-molecular backscatter coefficient (since BSR = (βaer + βmol) / βmol). The term "enhancement" instead typically refers to elevated values over a given background. Please revise this definition.

We agree. We replaced "BSR enhancement" with the standard terminology and now refer to $BSR_{455}-1$ as the aerosol backscatter ratio ($ABSR_{455}$).

> *To quantify model–measurement agreement for each profile, we compute (i) the Pearson correlation coefficient r between the area-normalized tracer-fraction profile and the COBALD aerosol backscatter ratio at 455 nm ($ABSR_{455}$), defined as BSR_{455}-1 (e.g., Cirisan et al., 2014; Reinares Martínez et al., 2021), over the main plume layer (375–450 K; 375–475 K on 30 September, 28 October, and 24 November 2019).*

Page 13, line 268: I cannot see "extreme" values in Fig. 7. Please quantify.

We replaced it with a quantitative statement and now report the peak-altitude mismatch in the control simulation.

> *Although the control simulation (orange lines) occasionally aligns with observed peak altitudes, its overall agreement is weaker and ~~it even generates unexplained extreme values on 12 August and 24 November.~~ it shows large peak-altitude biases on 12 August and 24 November 2019 ($|\Delta\theta\_peak| \approx 25$ K and ≈ 36 K, respectively; Fig. 7).*

Page 13, figure 6: it would be nice to show the tracer distribution over the Boulder site, since these simulations are also compared with the POPS data. Consider expanding the X-axis of Fig. 6 to include the entire Northern Hemisphere, or adding an extra figure focused on the American continent.

We thank the referee for this suggestion. As shown in our response to the major comments, we now include the tracer distribution over the Boulder site in the revised manuscript (Fig. 8).

Page 16, lines 304-309: I struggle to follow this paragraph and the argument of the "4-5 km additional lofting". If I understand correctly, this refers to the difference between the peak injection height of ~11 km derived from Cai et al. (2022), and the injection level inferred from the tracer simulation that best matches the observed profiles (400-420 K, i.e. 15-16.5 km). But how to be sure that this is due to radiative heating and not some other artifact/discrepancy between the different techniques? And what would be the time frame and the associated heating rates of the lofting? Since the plume has a large vertical extent (5-15 km), I would speculate that heating rates have a complex altitude dependency, so just comparing the peak height is not necessarily a good assumption. Unless this argument can be supported by a more detailed analysis, I think it should be presented as a speculation rather than a finding of the paper.

We agree and revised the paragraph accordingly. We now present radiative self-heating as a possible explanation for the vertical offset between the literature injection peak (~11 km) and the tracer level matching the observations (~15–16.5 km), but we clarify that injection-height estimates differ across techniques and are uncertain, so this comparison only provides a speculative interpretation rather than evidence for radiative lofting. Accordingly, we also removed the corresponding wording from the abstract and the conclusion, where it had been phrased as a finding.

> ~~*Based on the Lagrangian reconstruction by Cai et al. (2022), approximately 1.5 Tg of SO2 was initially injected between about 5 and 15 km, with a peak at around 11 km. If we use this central*~~

~~*injection altitude to estimate plume self-heating effects, the cloud may then be lofted by an additional ~ 4–5 km. Therefore, the height at which our SO2-based tracers best match observations will exceed the true injection center altitude. However, different observational techniques often report varying estimates of the injection center altitude (e.g., Kloss et al., 2021; Cai et al., 2022; Vernier et al., 2024). This also leads to uncertainty in our assessment of radiative lofting heights in this study.*~~ *Cai et al. (2022) estimate a peak injection altitude near 11 km, whereas the tracer level that best matches the observed profiles corresponds to ~15–16.5 km (400–420 K). We hypothesize that this ~4–5 km offset could be consistent with radiative self-heating lofting of the SO_2-rich cloud, but it may also reflect uncertainties in injection-height estimates across techniques and model-related discrepancies (e.g., Kloss et al., 2021; Cai et al., 2022; Vernier et al., 2024).*

Page 18, lines 333-334: what are exactly the "small-scale" and "often subgrid-scale" mixing processes?

We have removed this sentence as follow.

Our simulations show that ~~*small-scale atmospheric mixing processes are critical for dispersing the volcanic plume along its pathway through the stratosphere, and that representing these (often subgrid-scale) processes in models is essential for reliable simulations of volcanic plume transport.*~~ *atmospheric mixing processes, as parameterized in CLaMS in relation to flow deformation, are critical for dispersing the volcanic plume during stratospheric transport.*

Page 18, lines 336-337: I would appreciate a few statements on the overall relevance and fate of the volcanic aerosols entrained in the ASMA vortex, beyond the fact that this "may play an important role" in dispersing the aerosols. Is there a special relevance of this filament compared to the rest of the volcanic plume, e.g., in terms of more efficient aerosol transport to the stratosphere via the ASMA dynamics (see Vogel et al., 2019), higher cold-point tropopause, etc.? If so, this would be interesting to discuss.

We added a brief discussion clarifying that the plume fraction entrained into the ASMA is small. Based on established ASMA dynamics (e.g., Vogel et al., 2019), confinement and summertime diabatic uplift within the ASMA can potentially transport this fraction to higher altitudes in the UTLS, followed by redistribution and dilution. We revised the conclusions accordingly.

~~*In particular, our findings show that the ASMA may play an important role in dispersing aerosols from mid-latitude volcanic injections throughout the global stratosphere.*~~ *Our results suggest that a small fraction of the Raikoke plume becomes entrained into the ASMA. Within the ASMA, confinement and summertime diabatic uplift can potentially transport these plume fractions to higher altitudes (e.g., Vogel et al., 2019).*

Technical comments

Page 2, line 40: the full name of the volcano is "Hunga Tonga" or "Hunga Tonga-Hunga Ha'apai".

We revised the text to use the full volcano name ("Hunga Tonga") at first mention.

Page 3, line 72: replace "Section 7" with "Appendix A".

We have corrected “Section 7” to “Appendix A” .

Page 3, line 75: delete coordinates of Lhasa (already given).

Done

Page 5, line 105: the quantity e_{ice} (saturation vapor pressure over ice) is not defined.

where e_{ice} (T) is the saturation vapor pressure over ice at temperature T (in Kelvin), T_{mirror} is the measured frost-point temperature, and $T_{environment}$ is the ambient air temperature.

Page 5, line 114: delete "13 October" (not relevant).

We have removed the specific launch date (“13 October”)

TROPOMI, the satellite instrument aboard ESA’s sun-synchronous Sentinel-5P platform launched ~~on 13 October 2017~~ in 2017, is a hyperspectral imaging spectrometer …

Page 6, line 128: "an isentropic coordinate aligning layers" check grammar.

In the vertical direction it employs an isentropic coordinate ~~aligning layers with constant potential temperature θ,~~ that aligns the model layers with surfaces of constant potential temperature (θ) making the model well suited for stratospheric processes.

Page 11, line 211: add "of the plume" after "potential temperature".

~~Furthermore, the potential temperature measured by the satellite during its ASMA transit also closely matched the altitudes of enhanced BSR455 (Gorkavyi et al., 2021; Khaykin et al., 2022).~~ The potential temperature of the VVP during its transit through the ASMA inferred from satellite detections also closely matches the altitudes of enhanced BSR_{455} (Gorkavyi et al., 2021; Khaykin et al., 2022).

Page 12, lines 248-229: use the abbreviation of the Lyapunov exponent (λc) defined in Section 2.3.

Done

References (note: only papers not cited in the original manuscript are listed)

Brunamonti, S., Martucci, G., Romanens, G., Poltera, Y., Wienhold, F. G., Hervo, M., Haefele, A., and Navas-Guzmán, F.: Validation of aerosol backscatter profiles from Raman lidar and ceilometer using balloon-borne measurements, Atmos. Chem. Phys., 21, 2267–2285, https://doi.org/10.5194/acp-21-2267-2021, 2021.

Fahey, D. W., Gao, R.-S., Möhler, O., Saathoff, H., Schiller, C., Ebert, V., Krämer, M., Peter, T., Amarouche, N., Avallone, L. M., Bauer, R., Bozóki, Z., Christensen, L. E., Davis, S. M., Durry, G., Dyroff, C., Herman, R. L.,

Hunsmann, S., Khaykin, S. M., Mackrodt, P., Meyer, J., Smith, J. B., Spelten, N., Troy, R. F., Vömel, H., Wagner, S., and Wienhold, F. G.: The AquaVIT-1 intercomparison of atmospheric water vapor measurement techniques, Atmos. Meas. Tech., 7, 3177–3213, https://doi.org/10.5194/amt-7-3177-2014, 2014.

Park, M., Randel, W. J., Gettelman, A., Massie, S. T., and Jiang, J. H.: Transport above the Asian summer monsoon anticyclone inferred from Aura Microwave Limb Sounder tracers, J. Geophys. Res., 112, D16309, https://doi.org/10.1029/2006JD008294, 2007.

Poltera, Y., Luo, B., Wienhold, F. G., and Peter, T.: The “Golden Points” and nonequilibrium correction of high-accuracy frost point hygrometers, EGUsphere [preprint], https://doi.org/10.5194/egusphere-2025-2003, 2025.

Randel, W. J., Park, M., Emmons, L., Kinnison, D., Bernath, P., Walker, K. A., Boone, C., and Pumphrey, H.: Asian Monsoon Transport of Pollution to the Stratosphere, Science, 328, 611– 613, https://doi.org/10.1126/science.1182274, 2010.

Vogel, B., Müller, R., Günther, G., Spang, R., Hanumanthu, S., Li, D., Riese, M., and Stiller, G. P.: Lagrangian simulations of the transport of young air masses to the top of the Asian monsoon anticyclone and into the tropical pipe, Atmos. Chem. Phys., 19, 6007–6034, https://doi.org/10.5194/acp-19-6007-2019, 2019.

Original referee comments are in blue.

Our responses are in black with regular bold format. Text from the updated manuscript:

Appears in italic and with 0.5 cm indentation and with the modified parts in red.

General Comments:

This study presents comprehensive analyses of transport pathways of a rare volcanic eruption event and its impact on the stratospheric circulation by combining in-situ and satellite observations and global modeling. The results were reasonably structured throughout and well explained. However, most information in the main text seems to be focused rather on description of the results and lacks its significance or context. I think the authors should also emphasize the novelty of this work more clearly. A statement emphasizing how valuable in-situ measurements used in this study are and what can be achieved by using both the trajectory and global models can be included. I would also like to know if any studies that are similar to this work have ever done before. There are many places where the writings are vague. I would recommend improving clarity of writings to strengthen the paper's scientific quality.

We thank the reviewer for the constructive general and specific comments. In the revised manuscript, we strengthened the motivation and novelty statements, and expanded the discussion and conclusions to better highlight the broader implications for UTLS transport and ASMA circulation. We also clarified the value of the in-situ balloon-borne measurement and what can be achieved by combining trajectory analyses with global there dimensional tracer simulations, and added brief context on related studies. Finally, we revised the manuscript throughout to reduce vague wording and improve clarity. Specific changes are addressed point-by-point in our responses to the reviewer's specific comments below.

Specific Comments:

P1, L4: SO_2 -> sulfur dioxide (SO_2)

Done. We now write sulfur dioxide (SO_2) at first mention.

P1, L14: What does 'out-of-region' validation mean?

We clarified that "out-of-region validation" refers to evaluating the model with independent observations outside the ASMA region (here: Boulder, USA).

~~*Independent Portable Optical Particle Spectrometer (POPS) profiles over Boulder (USA) confirm the plume's timing and altitude, providing out-of-region validation.*~~ *Portable Optical Particle Spectrometer (POPS) profiles over Boulder (USA) confirm the plume's timing and altitude, providing an independent evaluation of its transport outside the ASMA region.*

P1, L15: 'Sensitivity…lofting' – The meaning of this sentence is unclear. Does this mean 'Sensitivity test using the CLaMS model indicates that the aerosols can be lifted additional ~4-5 km depending on the injection height due to aerosol-radiative lofting?

We agree that the original sentence was unclear. We have rephrased it to state that our CLaMS sensitivity tests show the best agreement with the observed profiles for tracer release

levels around 400–420 K (~15–16.5 km), which is about 4–5 km higher than the peak injection altitude (~11 km) reported by Cai et al. (2022). We now present aerosol radiative self-heating lofting as a possible explanation for this vertical offset, and we acknowledge that it may also reflect uncertainties in injection-height estimates and discrepancies between the model and the observational techniques. Accordingly, we removed wording that suggested radiative lofting as a conclusion of the paper.

P2, L18: It would be nice to add more recent work here, if there is any.

> *The impact of volcanic eruptions on climate has been a subject of widespread concern (McCormick et al., 1995; Thompson and Solomon, 2009; Solomon et al., 2011; Bourassa et al., 2012; Masson-Delmotte et al., 2021; Schmidt and Black, 2022).*
>
> *Masson-Delmotte, V., Zhai, P., Pirani, A., Connors, S. L., Péan, C., Berger, S., Caud, N., Chen, Y., Goldfarb, L., Gomis, M. I., Huang, M., Leitzell, K., Lonnoy, E., Matthews, J. B. R., Maycock, T. K., Waterfield, T., Yelekçi, O., Yu, R., and Zhou, B., eds.: Climate Change 2021: The Physical Science Basis, Cambridge University Press, Cambridge, United Kingdom and New York, NY, USA, https://doi.org/10.1017/9781009157896, 2021.*
>
> *Schmidt, A. and Black, B. A.: Reckoning with the rocky relationship between eruption size and climate response: toward a volcano-climate index, Annual Review of Earth and Planetary Sciences, 50, 627–661, 2022.*

P2, L26: negative -> negative radiative

Done.

P2, L31: from an eruption -> from an eruption are

Done.

P2, L35: There should be something at the end of this sentence. ‘far longer than xxx’.

Done. We completed the sentence by specifying the comparison (longer than tropospheric plumes).

> *Eruption products injected directly into the stratosphere—or volcanic plumes in the upper troposphere that self-loft via radiative heating into the lower stratosphere—can persist far longer than plumes confined to the troposphere.*

P2, L36: It needs a reference for the Brewer-Dobson circulation here.

Done. We added a reference for the Brewer–Dobson circulation.

> *Aerosols from tropical eruptions are transported most efficiently via the Brewer–Dobson circulation (Brewer, 1949; Dobson, 1956; Butchart, 2014), whereas mid-latitude eruption aerosols can still reach the tropics through Rossby-wave breaking or transport by the Asian Summer Monsoon Anticyclone (ASMA) (Konopka et al., 2009; Kloss et al., 2021; Wu et al., 2023).*
>
> *Brewer, A. W.: Evidence for a world circulation provided by the measurements of helium and water vapour distribution in the stratosphere, Q. J. R. Meteorol. Soc., 75, 351–363, https://doi.org/10.1002/qj.49707532603, 1949.*

Dobson, G. M. B.: Origin and distribution of polyatomic molecules in the atmosphere, Proc R Soc London A, 236, 187–193, 1956.

Butchart, N.: The Brewer-Dobson circulation, Rev. Geophys., 52, 157–184, https://doi.org/10.1002/2013RG000448, 2014.

P2, L42-44: Among…summer. Deep…circulation -> These need to be supported by references.

We agree. We have removed the original phrasing and reorganized the text to more clearly emphasize the ASMA's role in boreal-summer UTLS transport, supported by appropriate references.

In the Northern Hemisphere summer, the ASMA is the dominant circulation system in the UTLS. Deep convection injects pollutants into the UTLS, where the ASMA's strong anticyclonic circulation acts as a dynamical transport barrier, confining these air masses over Asia during ascent into the stratosphere (e.g., Park et al., 2007; Randel et al., 2010; Fadnavis et al., 2014; Santee et al., 2017; Vogel et al., 2019). However, as the ASMA boundary is not a strict transport barrier, air masses can be exported from the monsoon circulation into the extratropical UTLS (Vogel et al., 2016; Yu et al., 2017). This combination of confinement and export is important for interpreting aerosol dispersion during boreal summer, including the dispersion of volcanic aerosol.

P3, L52: How was June 21-22 period determined to be during the anticyclone's mature phase?

Thank you for the comment. We clarified that "mature phase" refers to August 2019, when the Raikoke plume is transported into and through the ASMA (the period relevant to our balloon observations), rather than to the eruption dates (21–22 June 2019).

~~*The mid-latitude Raikoke volcano (48◦ N, 153◦E) erupted on 21–22 June 2019 (VEI 4), and its aerosol plume was advected through the ASMA during the anticyclone's mature phase, providing an ideal case to examine how the ASMA modulates volcanic plume transport*~~. *The mid-latitude Raikoke volcano erupted on 21–22 June 2019. …. In August 2019, part of the aerosol plume was transported into and through the ASMA during the mature stage of the boreal-summer anticyclone, providing an ideal case to examine how the ASMA modulates volcanic plume transport.*

P3, L56-58: The…plumes. -> Are these also in Khaykin et al. (2022)?

Yes. We added the appropriate reference (Khaykin et al., 2022).

Three days after the eruption, compact anticyclonic "vorticized volcanic plumes" (VVPs) detached from the main volcanic cloud, trapping more than half of the SO_2 mass (Khaykin et al., 2022). The primary VVP then rose to ∼27 km, spanning ∼400 km in width but only ∼1.5 km in depth. Meanwhile, the residual main plume was diluted at lower altitudes, resulting in two distinct Raikoke plumes (Khaykin et al., 2022).

P3, L59: when the site…levels. -> This sentence needs to be more specific. Was this based on the measurements of a specific variable, such as, geopotential height?

Yes, we now specify that the ASMA position is indicated using ERA5 geopotential height at 150 hPa and we added the corresponding contour in Figure 1 (Figure 1a of the manuscript). The text and caption have been revised accordingly.

Beginning in August 2019, frequent balloon-borne measurements were conducted over Lhasa (29.66◦N, 91.14◦ E), ~~*when the site lay inside the ASMA at UTLS levels.*~~ *which was located within the ASMA at UTLS levels, as indicated by the ERA5 150 hPa geopotential height field (Fig. 1a).*

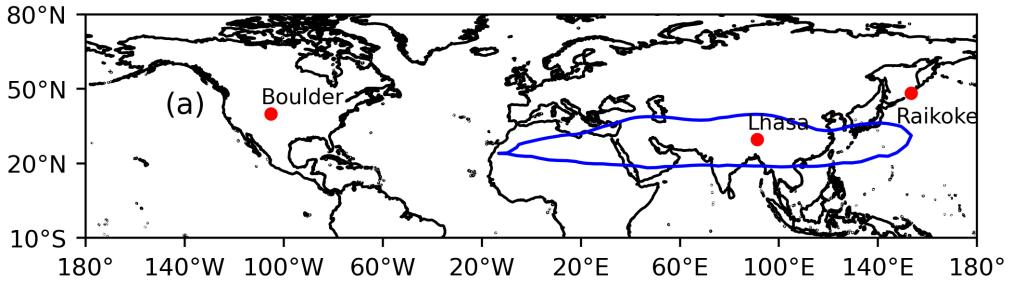

Figure 1 (Figure 1a of the revised manuscript). Map showing the locations of the balloon measurement sites over Lhasa (29.7°N, 91.1°E) and Boulder (39.9°N, 105.2°W), and the Raikoke volcano (48.3°N, 153.3°E). The blue contour shows the ERA5 geopotential height at 150 hPa averaged over August 2019 at 00 UTC. The 14.32 km contour is used here as an indicator of the ASMA at UTLS levels.

P3, L64: from the TROPOsperic Monitoring Instrument (TROPOMI)

Done.

from the Tropospheric Monitoring Instrument (TROPOMI) aboard Sentinel-5P (Theys et al., 2024).

P3, L65: from Lhasa and Boulder -> Are those measurement locations? Why was Boulder selected here?

Yes, Lhasa and Boulder are the measurement locations. Boulder was included as an independent site outside the ASMA region to assess the plume evolution and its transport within the Northern Hemisphere, and to provide an external evaluation of the CLaMS simulations.

~~*We also incorporate Portable Optical Particle Spectrometer (POPS) measurements from Lhasa (Tibet) and Boulder (USA).*~~ *We further use POPS profiles from Lhasa and Boulder to evaluate the simulated plume evolution over the Northern Hemisphere. In particular, Boulder serves as an independent site outside the ASMA region to evaluate plume transport.*

P3, L67: I think the authors should state that why their work is new and how it is different from the previous studies. I think scarcity of in-situ measurements for the Raikoke or any volcanic eruption should be mentioned here.

We agree and have added a brief statement on the novelty and the limited availability of in situ UTLS measurements for the 2019 Raikoke eruption. We highlight that our study combines rare balloon-borne measurements with high-resolution ERA5-driven CLaMS trajectories and global SO_2-based tracer simulations, which together provide observational constraints on transport pathways, timing, and plume dilution in the ASMA.

~~*This study investigates how the ASMA modulates UTLS volcanic plume transport following the Raikoke eruption.*~~ *In situ UTLS observations of volcanic aerosol are rare, particularly for the 2019 Raikoke eruption. Here we combine balloon-borne COBALD and POPS profiles with high-*

resolution ERA5-driven CLaMS backward trajectories and global three-dimensional SO_2-based tracer simulations to identify transport of the Raikoke plume through the Northern Hemisphere and into the ASMA, with particular attention to transport pathways and time scales.

P3, L75: Please include exact days of the SWOP campaign. Also, why were the ECC measurements not analyzed?

We have added the exact balloon launch dates (Table 1 in the revised manuscript) for the SWOP measurements used in this study. ECC ozone data are not analyzed because this paper focuses on aerosol plume identification and transport using COBALD and POPS; ozone analysis is beyond the scope of the present work.

Site	Flight ID	Date	Mid-ascent time (UTC)	Key instruments	Observed plume layer: θ (K)	Observed plume layer: p (hPa)
Lhasa	F01	30.07.19	17:58	COBALD CFH	–	–
	F02	01.08.19	15:45	COBALD CFH	–	–
	F03	03.08.19	15:23	COBALD CFH	410–422; 459–472	78–71; 59–56
	F04	06.08.19	15:26	COBALD CFH	404–416	82–75
	F05	08.08.19	15:10	COBALD CFH	389–423	98–73
	F06	10.08.19	16:05	COBALD CFH	397–422	84–70
	F07	12.08.19	15:49	COBALD CFH	398–426	84–71
	F08	15.08.19	17:24	COBALD CFH	406–423	79–71
	F09	20.08.19	17:14	COBALD CFH POPS	393–434	89–68
	F10	30.09.19	15:34	COBALD CFH	385–452	96–64
	F11	28.10.19	15:24	COBALD CFH	390–459	100–60
	F12	24.11.19	15:09	COBALD CFH	410–482	79–55
	F13	04.01.20	15:29	COBALD CFH	393–399; 415–432	118–115; 99–91
Boulder	F14	28.06.19	17:05	POPS	–	–
	F15	07.08.19	17:08	POPS	373–442	122–73
	F16	27.08.19	16:38	POPS	385–429; 480–505	117–80; 59–52
	F17	08.11.19	17:58	POPS	389–435	107–76
	F18	03.12.19	18:05	POPS	–	–

Table 1 (revised manuscript). Summary of analyzed balloon flights at Lhasa and Boulder, including sequential flight ID, date, mid-ascent time (UTC), key instruments used in this study, and the potential temperature (θ) and pressure (p) ranges of the observed volcanic plume layer. The plume layer was identified from COBALD measurements where $BSR_{455} > 1.1$ and $CI > 6$, and from POPS measurements where the particle number concentration exceeded 150 cm^{-3}. Mid-ascent time denotes the midpoint of the ascent period from launch to balloon burst. The "Key instruments" column lists only the instruments analyzed in this work; additional payload components were flown but are not listed here. A dash (-) denotes that no volcanic plume layer was identified for that flight.

P3, L81: Please add information about location of the ASMA relative to Lhasa during July-August 2019. As an option, a contour of a geopotential height can be added in Fig. 1a.

Please see our response to P3, L59. We added the ERA5 150 hPa geopotential height contour in Fig. 1a to show the ASMA location relative to Lhasa and updated the figure caption accordingly.

P5, L103: A citation is needed for the iMet radiosonde.

Done. We now specify the radiosonde as an International Met Systems (InterMet) iMet-1-RSB and added a reference to the manufacturer documentation at first mention.

> *Balloons were equipped with an electrochemical concentration cell (ECC) ozonesonde, a cryogenic frostpoint hygrometer (CFH), a compact optical backscatter aerosol detector (COBALD), and an International Met Systems (InterMet) iMet-1-RSB radiosonde (GRUAN Lead Centre, 2025). ECC measurements are not analyzed in this study.*
>
> *GRUAN Lead Centre: InterMet iMet-1 (iMet-1-RSB) — GRUAN instrument information (radiosonde models), https://www.gruan.org/instruments/radiosondes/sonde-models/intermet-imet-1, accessed 13 Jan 2026, 2025.*

P5, L110: Is 'sizing' referring to aerosol particles sizing?

Yes. Here, "sizing" refers to particle sizing (the conversion from scattering signal to particle diameter). We clarified this in the text.

> *Measurement uncertainties are dominated by particle sizing (including sensitivity to the assumed refractive index) and flow-rate calibration (Gao et al., 2016).*

P5, L121: …limit are excluded following Theys et al. (2024).

We clarified that values below 0.3 DU are excluded following Theys et al. (2024).

> *…values below the instrument's 0.3 DU detection limit are excluded, following Theys et al. (2024).*

P6, L127: 'applied' can be substituted with 'used'.

Done. We replaced "applied" with "used".

> *CLaMS is ~~applied~~ used here to investigate the transport of the volcanic plume following the Raikoke eruption.*

P6, L129: hybrid coordinate -> hybrid coordinate

We revised this sentence for clarity.

> *The CLaMS ~~vertical coordinate – the hybrid coordinate ζ –~~ hybrid vertical coordinate (ζ) follows orography near the surface and transitions smoothly into θ once σ = p / psurf reaches 0.3 (usually about 300 hPa) (Pommrich et al., 2014).*

P6, L132: main runs -> control runs

We replaced "main runs" with "standard runs" to clarify that the native hourly 0.3° × 0.3° ERA5 forcing is our standard configuration.

> *…the ~~main~~ standard runs use the native hourly fields on the 0.3° × 0.3° grid with 137 vertical levels up to 80 km (Hersbach et al., 2020), whereas …*

P6, L132: 0.3º x 0.3º (latitude x longitude)

Done. We clarified that the 0.3° × 0.3° grid refers to latitude × longitude.

> *…on the 0.3° × 0.3° (latitude × longitude) grid…*

P6, L134 (and elsewhere): 6 h -> 6 hours
Done. We replaced "6 h" with "6 hours" throughout.

L6, L147: what does 'tracer injection mask' mean? Is this term used in CLaMS modeling in general?

By "tracer injection mask" we mean the 0/1 geographic source region used to initialize the tracer (value 1 inside the selected SO_2 plume area and 0 outside) at the injection time. We clarified this definition in the text and use "source-region mask" in the revision for clarity.

> ~~*…as the tracer injection mask; only the spatial extent, not the column amplitude, was used.*~~*as a 0/1 source-region mask for tracer initialization (1 inside the selected SO_2 plume area, 0 outside); only the spatial extent, not the column amplitude, was used.*

P7, L158: Briefly explain why this method is practical.

We added a brief explanation that the method is practical because it combines collocated backscatter (COBALD) and humidity (CFH), allowing a straightforward distinction between ice clouds and aerosol layers in situ.

> *The COBALD–CFH tandem provides a practical method for identifying cirrus clouds and aerosol layers because collocated backscatter and frost-point humidity measurements allow a straightforward separation of ice-cloud signatures from aerosol enhancements (Brabec et al., 2012; Cirisan et al., 2014; Reinares Martínez et al., 2021; Yang et al., 2023).*

P7, L165: What does 'empirically highlighted' mean?

Thank you for the comment. We agree that the phrase "empirically highlighted" was unclear. We have replaced it with a description of the objective selection criteria: cirrus is excluded using $BSR_{455} > 1.2$, $RH_{ice} > 70\%$, and CI > 7; aerosol layers are then defined by $BSR_{455} > 1.1$ and classified using CI = 6 (Raikoke plume: CI > 6; ATAL/background: CI < 6).

P7, L174: …differs markedly… -> Could this be 'is significantly higher'?
The phrase "differs markedly" was not intended to emphasize the peak position, but rather the peak magnitude. We have revised the text to clarify that the more robust difference is the higher median BSR455 peak in 2019 (about 1.25) compared with the 2013 ATAL peak (about 1.10), while the higher potential temperature of the 2019 peak is retained as supporting information.

> *In general, ATAL-related enhancements in COBALD BSR_{455} profiles are largely confined to 360–400 K (core near 370–390 K), with occasional extensions up to 420–440 K depending on region and year (Vernier et al., 2015, 2018; Appel et al., 2022). The ATAL profile from 2013 shown in Fig. 3a is taken from the COBALD measurements over Lhasa reported by Vernier et al. (2015). The 2019 median peak occurs near 417 K, about 33 K above the 2013 ATAL peak (384 K), corresponding to roughly 1.7 km in altitude in the UTLS (based on the 30 July 2019 background sounding). The vertical extent of ATAL enhancements varies across regions and years; therefore, we emphasize the peak magnitude as the more robust difference: the 2019 Raikoke-related median BSR_{455} reaches ∼1.25, exceeding the 2013 ATAL peak (∼1.10; Fig. 3a).*

P7, L178: Why was the particle number density over Boulder so high in August? I think the impact of large-scale global circulation transporting aerosols between Lhasa and Boulder should be explained.

Thank you for the comment. Our global three-dimensional CLaMS tracer simulations (Sect. 4.2) show that the main Raikoke plume is transported predominantly along the subtropical westerly jet in the mid-latitude UTLS. Boulder lies closer to this main transport corridor, whereas Lhasa is located within the ASMA, where the anticyclonic circulation acts as a partial horizontal transport barrier. As a result, the plume fraction reaching Lhasa represents a more limited filament of the plume, which helps explain why POPS number densities at Boulder can be higher than at Lhasa in August. We added a short clarification in the text.

> *The particle number density at Lhasa on 20 August was lower than that at Boulder on 7 August and 27 August. This is consistent with the global CLaMS tracer simulations (Sect. 4.2; cf. Figs. 7 and 8), which show that the main Raikoke plume is transported along the subtropical westerly jet in the mid-latitude UTLS, while transport into the ASMA interior is more limited due to the anticyclone acting as a partial horizontal barrier. Section 4 presents backward-trajectory calculations and three-dimensional tracer simulations with CLaMS to verify the origin and transport pathways of the plume observed over Lhasa and Boulder.*

P9, L187: Is the 'eruption period' same as 21-22 June 2019?
We use a single reference time as the endpoint for the backward trajectories, 21 June 2019 at 18:00 UTC, rather than the full 21–22 June eruption period. We clarified this in the text.

> *~~Backward trajectories were launched every second along the balloon's vertical ascent in the potential temperature range where an enhanced BSR455 was observed in Fig. 2, and traced back to the eruption period.~~ All trajectories were calculated backward to a single common reference time (21 June 2019, 18:00 UTC), which serves as the trajectory endpoint for all cases.*

P10, Fig. 4: It is hard to understand the direction of transport in this figure. Is the air moving mostly to the East from the eruption location? Also, what is the unit of x-axis? It looks like x-axis has irregular intervals, which makes it hard to understand.

Thank you for the comment. We have revised the figures as follows. Figure 2 (Figure 4 of the revised manuscript) shows backward trajectories; we clarified the time axis by labeling it as Date (dd.mm.yy) and by updating the caption to state that the x-axis represents the backward integration from the balloon initialization time back to the eruption reference time.

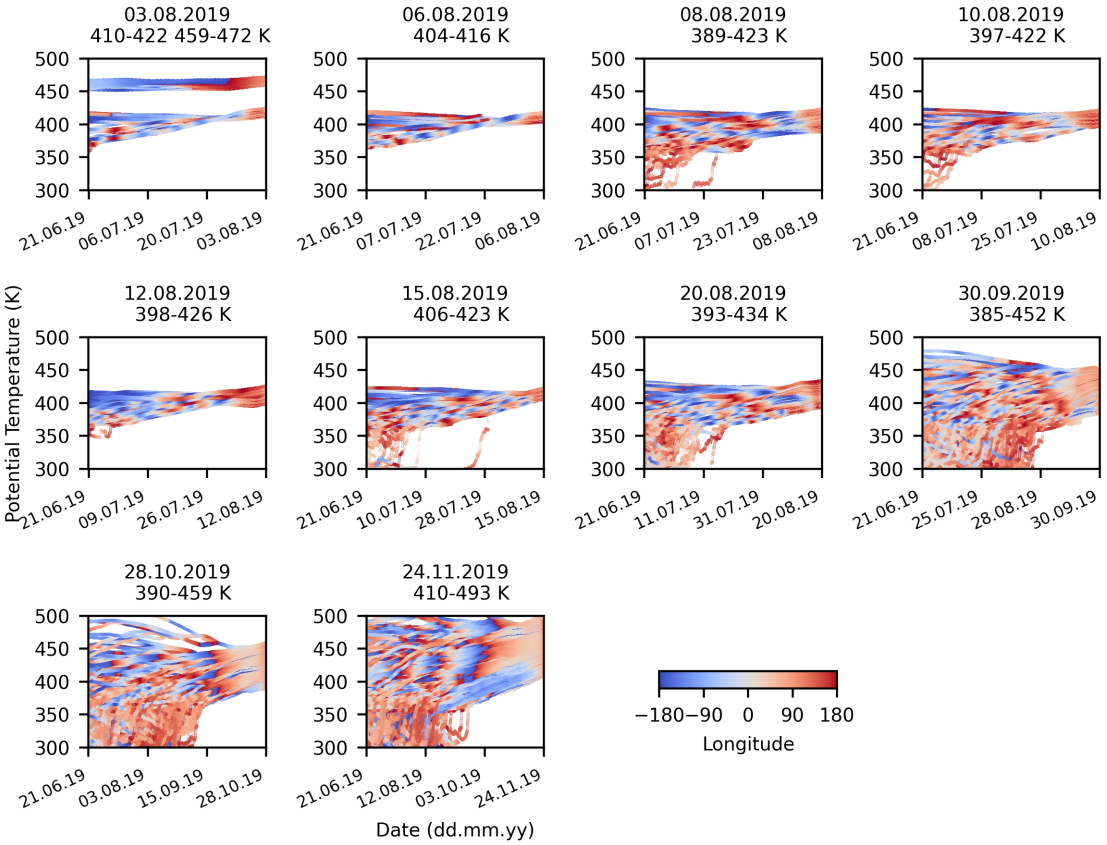

Figure 2 (Figure 4 of the revised manuscript). Backward trajectories initialized from the Lhasa balloon observations and traced back to the Raikoke eruption reference time (21 June 2019, 18:00 UTC). Only trajectories initialized within the enhanced BSR455 potential-temperature range (orange shading in Fig. 2) are shown. Colors indicate trajectory longitude. The x-axis shows date (dd.mm.yy) along the backward integration (right: balloon initialization time; left: eruption reference time).

P11, L211: Which satellites were used in these studies?

We clarified this in the text. The satellite observations in Gorkavyi et al. (2021) and Khaykin et al. (2022) are primarily based on TROPOMI on Sentinel-5P.

~~*Furthermore, the potential temperature measured by the satellite during its ASMA transit also closely matched the altitudes of enhanced BSR455 (Gorkavyi et al., 2021; Khaykin et al., 2022).*~~ *The potential temperature inferred from TROPOMI (Sentinel-5P) plume detections during the ASMA transit also closely matched the altitudes of enhanced BSR_{455} (Gorkavyi et al., 2021; Khaykin et al., 2022).*

P11, L215-217: This is somewhat vague. I would suggest revising it with more specific information for clarity.

We agree and revised this sentence to specify the two branches and their controlling circulation regimes.

~~*Although both sets of air parcels correspond to the same balloon-borne observation profile, they represent entirely different transport pathways – originating from two distinct regions of the Raikoke plume at different altitudes and driven by different processes.*~~ *Although both sets of air parcels belong to the same balloon profile, they trace back to two distinct plume components:*

the l lower-θ main plume in the subtropical westerly jet (~410–422 K) and the higher- θ VVP filament in the summertime easterlies (~459–472 K). This indicates different source altitudes within the Raikoke plume and distinct dynamical transport pathways.

P11, L223 (and elsewhere): What do 'SO_2-based tracers' mean?

By "SO_2-based tracers" we mean passive tracers initialized from the observed SO_2 plume mask (1 inside, 0 outside) at the injection time and then transported and mixed in CLaMS. We clarified this in the text.

In the global three-dimensional CLaMS simulations, ~~SO_2-based tracers were released within the defined region (Fig. 1b) at potential-temperature levels of 400–420 K at 00:00 UTC on 25 June 2019 to simulate the dispersal of the volcanic plume.~~ we use passive tracers initialized from the observed SO_2 plume mask (Fig.~1b). We refer to these as SO_2-based tracers. At 00:00 UTC on 25 June 2019, the tracer is set to 1 inside the mask (0 outside) within three potential-temperature ranges (380–400 K, 400–420 K, and 420–440 K) and then advected and mixed throughout the global atmosphere in CLaMS.

P11, L225: global maps with -> global maps of?

Done.

Figure 7 shows global maps of fractions of the SO_2-based tracers falling within the 400–420 K layer for each measurement day from 30 July to 20 August 2019, using the modified simulation.

P12, L231: the dynamical situation…-> the isentropic transport, showing outflow of the ASMA and in-mixing…

Done. We revised the wording to refer to isentropic transport and to describe ASMA outflow and in-mixing more directly.

The 11 PVU potential vorticity contour (layer mean over 400–420 K) ~~indicates the dynamical situation, showing in addition outflow of the ASMA (filaments) and in-mixing of PV-rich air from high latitudes.~~ illustrates the isentropic transport, including ASMA outflow (filaments) and in-mixing of PV-rich air from high latitudes.

P12, L234: Which 'observations' specifically?

We clarified that this refers to the Lhasa balloon observations (COBALD profiles) used in this study.

The results shown in Fig. 6 illustrate the overall intrusion of air masses into the ASMA and agree well with the Lhasa COBALD BSR_{455} observations.

P12, L244: How does 'Lyapunov exponent' work in CLaMS?

We added a short explanation in the revised manuscript (Sect. 2.3). In CLaMS, parameterized mixing is triggered when the integral deformation between neighboring air parcels exceeds the critical value $\gamma c=\lambda c\,\Delta t$, where λc is the critical Lyapunov exponent and Δt is the mixing interval. Thus, for a given Δt, a larger λc (larger γc) implies less frequent parameterized mixing (and vice versa).

In the CLaMS mixing scheme, parameterized mixing is triggered when the integral deformation between neighboring air parcels exceeds an empirical critical deformation γc = Δt Δt, where λc is the critical Lyapunov exponent and Δt is the advective time step (mixing interval). For a given Δt, a larger Δt (thus a larger γc) requires stronger deformation to trigger mixing and therefore corresponds to less frequent parameterized mixing (and vice versa) (Konopka et al., 2004, 2007). In our setup, the modified simulation corresponds to enhanced parameterized mixing compared to the control simulation. Throughout most of the paper we show results from the modified simulation, as these agree better with the observations. Sensitivity to parameterized mixing intensity and comparisons with the control simulation are discussed in Sect. 5.1. The mixing configurations and the additional sensitivity runs (rectangular mask and coarser ERA5 input) are summarized in Table 2.

P12, L252: driving data -> either change to 'input' or remove it

Done. We revised this sentence.

~~*Note that, for the control simulation, changing the resolution of the ERA5 driving data has only a minor effect and does not affect our conclusions; compare Fig. A1 (0.3◦ × 0.3◦ resolution, 1 hours) with Fig. A2 (1◦ × 1◦ resolution, 6 hours).*~~ *However, changing the ERA5 resolution has only a minor effect and does not affect our conclusions. This is evident from the comparison of Fig. A1 (0.3◦ × 0.3◦ resolution, 1 hours) and Fig. A2 (1◦ × 1◦ resolution, 6 hours).*

P14, L279-284: What is the significance of this result in terms of large-scale circulation?

These Boulder comparisons provide an independent evaluation outside the ASMA, showing that the modified simulation represents the timing and altitude of the Raikoke plume in the mid-latitude UTLS more reliably. This supports our interpretation that transport and dispersion along the large-scale mid-latitude circulation (including the subtropical jet and subsequent mixing) are sensitive to the representation of mixing, and that the modified configuration yields the most consistent large-scale evolution.

Over Boulder, we likewise compare the tracer-fraction profiles on the measurement dates with the POPS aerosol number concentration profiles at STP (Fig. 10). For the computation of r, we evaluate within 375–450 K for 7 August and 27 August 2019, and within 375–475 K for 8 November 2019. Overall, the SO_2-based tracers in the modified simulation (blue) reproduce the observed peak structure more closely, with higher r and smaller $|\Delta\theta|$ than the control and rectangle-based simulations. This indicates that the plume evolution along the mid-latitude UTLS circulation is sensitive to the representation of mixing, and that the modified configuration better captures the large-scale transport and dispersion.

P15, L286: How long did the initial injection last?

We added the duration of the main injection: 21 June 2019 18:00 to 22 June 2019 03:00 UTC (about 9 hours), noting that some reconstructions extend SO_2 release to ~06:00 UTC.

The Raikoke plume was injected primarily within 8–16 km (Kloss et al., 2021; Cai et al., 2022; Vernier et al., 2024). The main injection occurred between 18:00 UTC on 21 June and 03:00 UTC on 22 June 2019 (with SO_2 release possibly extending to ~06:00 UTC) (Cai et al., 2022; Vernier et al., 2024).

P15 (Figs. 7-10): The locations and dates are not easy to see on these figures. I recommend either using larger size fonts or placing them on them the title.

Done.

P16, L307-309: The relevance of these two sentences to this study is unclear.

We have revised the paragraph to state that the ~4–5 km vertical offset is only a possible interpretation (e.g., radiative self-heating lofting), and that it may also arise from uncertainties in injection-height estimates and model/technique differences. The text has been rephrased accordingly.

> ~~*Based on the Lagrangian reconstruction by Cai et al. (2022), approximately 1.5 Tg of SO2 was initially injected between about 5 and 15 km, with a peak at around 11 km. If we use this central injection altitude to estimate plume self-heating effects, the cloud may then be lofted by an additional ~ 4–5 km. Therefore, the height at which our SO2-based tracers best match observations will exceed the true injection center altitude. However, different observational techniques often report varying estimates of the injection center altitude (e.g., Kloss et al., 2021; Cai et al., 2022; Vernier et al., 2024). This also leads to uncertainty in our assessment of radiative lofting heights in this study.*~~ *Cai et al. (2022) estimate a peak injection altitude near 11 km, whereas the tracer level that best matches the observed profiles corresponds to ~15–16.5 km (400–420 K). This ~4–5 km offset could be consistent with radiative self-heating lofting of the SO_2-rich cloud, but it may also reflect uncertainties in injection-height estimates across techniques and model-related discrepancies (e.g., Kloss et al., 2021; Cai et al., 2022; Vernier et al., 2024).*

P17, L311: A motivation for this study can be stated here as well.

Done. We added a brief motivation sentence at the beginning of the Conclusions.

> *Motivated by the limited availability of in-situ UTLS measurements of volcanic plume transport and the need to better quantify ASMA-related pathways, we combined in-situ balloon observations over Lhasa and Boulder with Lagrangian transport simulations using the CLaMS model, driven by high-resolution ERA5 data, to investigate the transport pathways and mixing processes of the Raikoke plume in the UTLS during the mature phase of the ASMA. Our main conclusions are:*

P17, L337: What is the significance of the results in understanding role of volcanic eruption in our climate?

We added a brief statement in the Conclusions on climate relevance.

> *In summary, by combining observations and modelling, we provide further insights into how the mid-latitude Raikoke plume is transported through the Northern Hemisphere UTLS over long distances. We show evidence that the Asian summer monsoon plays a key role in this transport. In particular, parts of the plume are entrained into the monsoon anticyclone and are subsequently diluted by horizontal transport and vertical upwelling within the anticyclone. Our findings improve the understanding of how aerosols from a mid-latitude volcanic injection are transported and dispersed in the lower stratosphere, including in the vicinity of the Asian summer monsoon. This improved understanding of plume transport and dilution is relevant for*

estimating regional radiative forcing and assessing potential impacts on stratospheric ozone chemistry.

~~*We identified two distinct isentropic transport pathways and quantified the dilution mechanism via mixing from air masses outside the plume. Our simulations show that small-scale atmospheric mixing processes are critical for dispersing the volcanic plume along its pathway through the stratosphere, and that representing these (often subgrid-scale) processes in models is essential for reliable simulations of volcanic plume transport. In this sense, changes in model resolution require adjustment of mixing parameterizations. In particular, our findings show that the ASMA may play an important role in dispersing aerosols from mid-latitude volcanic injections throughout the global stratosphere.*~~ *We identified two distinct isentropic transport pathways and assessed plume dilution via mixing with air masses outside the plume. Our simulations show that atmospheric mixing processes, as parameterized in CLaMS in relation to flow deformation, are critical for dispersing the volcanic plume during stratospheric transport. Accordingly, changes in model resolution require adjustment of the mixing parameterization. Our results suggest that a small fraction of the Raikoke plume becomes entrained into the ASMA. Within the ASMA, confinement and summertime diabatic uplift can potentially transport these plume fractions to higher altitudes (e.g., Vogel et al., 2019).*